

# Quantitative insights into energy contributions of intermolecular interactions in fluorine and trifluoromethyl substituted isomeric *N*-phenylacetamides and *N*-methylbenzamidest

Cite this: *CrystEngComm*, 2013, 15, 3711

Piyush Panini and Deepak Chopra\*

The presence of the C–F bond in organic molecules, particularly in the context of generating different intermolecular interactions of the type C–F⋯F–C, C–H⋯F and C–F⋯π is of extreme significance in the realm of structural chemistry. These interactions generate different packing motifs in the formation of the crystal. It is of interest to evaluate the energetic contributions of such weak interactions to evaluate their important role in crystal packing. In this respect, a library of twelve compounds containing a strong donor and acceptor, along with the presence of a C–F bond in different electronic environments (fluorine atom connected to C(sp<sup>2</sup>) and C(sp<sup>3</sup>) carbon atom) have been synthesized and characterized using single crystal X-ray diffraction studies at low temperature. In addition, the non-fluorinated counterpart has also been synthesized. These crystal structures have been analyzed to understand the contribution of weak interactions involving organic fluorine in the crystal packing. Furthermore, the stabilizing–destabilizing roles of such interactions in terms of favourable energetics have been quantified with inputs from calculations performed using PIXEL. It is observed that most of the interactions involving fluorine are of a dispersive character, and in some cases the interaction is also coulombic in origin. These results have been compared with *ab initio* quantum-chemical calculations (DFT-D3/B-97D level) performed using TURBOMOLE. In addition, the lattice energies of all the compounds have been evaluated, and the total contribution partitioned into the corresponding coulombic, polarization, dispersion and exchange contributions using the CLP module. The results correlate well with thermochemical data experimentally determined for these compounds.

Received 29th October 2012,  
Accepted 26th February 2013

DOI: 10.1039/c3ce40111a

www.rsc.org/crystengcomm

## Introduction

In recent years, the determination of accurate crystal and molecular structures has become a routine process. The Cambridge Structural Database<sup>1</sup> is a well-established storehouse of such determinations for compounds that are solids at room temperature. In recent years, the focus has also shifted towards the investigation of crystal structures of compounds that are liquids at room temperature.<sup>2</sup> Most of the crystallographic analysis that follows from structure determination involves interpretation of the molecular geometry and a working knowledge of a variety of intra- and intermolecular interactions on pure geometrical considerations. The missing link is to explore the energetics associated with these interactions, particularly intermolecular ones, which provide

a platform for the molecules to associate with each other.<sup>3</sup> In this regard, the role of strong intermolecular H-bonds of the type N–H⋯O, O–H⋯O and O–H⋯N is already well established<sup>4</sup> in addition to weak C–H⋯π<sup>5</sup> and π⋯π interactions.<sup>6</sup> The presence of halogens in organic molecules generates a variety of interactions of the type C–X⋯X–C,<sup>7a</sup> C–X⋯O,<sup>7b</sup> C–H⋯X<sup>7c</sup> and C–X⋯π.<sup>8</sup> The interactions in heavier halogens have been well-investigated from a topological analysis of the electron densities in crystalline solids.<sup>9</sup> Of particular interest in this context are intermolecular interactions of organic fluorine, which have been postulated to be weak H-bond acceptors, primarily associated with high electronegativity and tightly contracted lone pairs of electrons.<sup>10</sup> In the last decade, there have been innumerable crystallographic reports on structure determinations in organic compounds containing organic fluorine.<sup>11</sup> A recent article<sup>12</sup> brings out the significance of hydrogen bonds with fluorine with detailed inputs from studies performed in solution, gas phase and in the crystal in fluorine containing compounds. A recent review,<sup>13</sup> highlight,<sup>14</sup> book<sup>15</sup> and a perspective<sup>16</sup> brings out the versatility

Department of Chemistry, Indian Institute of Science Education and Research  
Bhopal, ITI (Gas Rahat) Building, Bhopal 462023, India.  
E-mail: dchopra@iiserb.ac.in; Fax: +91 0755-4092-392

† Electronic supplementary information (ESI) available. CCDC 907077–907090.  
For ESI and crystallographic data in CIF or other electronic format see DOI:  
10.1039/c3ce40111a

associated with interactions involving organic fluorine. A topological analysis of the electron density in fluorine containing solids reveal that C–H...F interactions have weak H-bonding characteristics.<sup>17</sup> In a recent study, short and directional C–H...F intermolecular interactions in the absence of strong H-bond donors have been observed in mono- and difluorinated imines.<sup>18</sup> The energetic stabilization of such weak C–H...F interactions are in the range of 1.0–5.0 kcal mol<sup>-1</sup> and these contribute towards the stability of the crystal packing. Similar calculations on fluorinated pyridines also bring out the subtle effects associated with such interactions.<sup>19</sup> In order to evaluate the importance of cooperativity in interactions in crystalline solids, it was of interest to investigate weak C–H...F intermolecular interactions in the presence of strong hydrogen bond donors and acceptors. Such detailed crystallographic investigations have already been performed in mono- and difluorinated benzanilides,<sup>20</sup> homo and hetero halogen substituted benzanilides,<sup>20b</sup> and mono- and di-trifluoromethylated benzanilides.<sup>20c</sup> In all the above-mentioned systems, the library of compounds synthesized have been so chosen so as to investigate the nature of interactions in halogen containing compounds containing a strong H-bond donor, namely N–H and a strong acceptor, *i.e.* the C=O group. These systems contain only one type of hydrogen atom, all being connected to the aromatic ring. In our present study, the chemical nature of the synthesized compounds is modified in comparison to the previously investigated compounds. In addition to containing a peptide bond (of significance in biomolecules and proteins), the current library of synthesized molecules contain two types of fluorine and hydrogen atoms in different electronic environments. In one case, the fluorine atom is connected to an sp<sup>2</sup> carbon (a part of an aromatic ring) and in the other case it is connected to the sp<sup>3</sup> carbon (a part of the trifluoromethyl group). The electron density on the fluorine atoms is more a case of the latter due to lack of resonance effects with the benzene nucleus. The hydrogen atoms are of different types, one constituting the benzene nucleus and the other consisting of a methyl group. This allows for an investigation into the geometrical and energetic features associated with weak C(sp<sup>3</sup>/sp<sup>2</sup>)–H...F–C(sp<sup>3</sup>/sp<sup>2</sup>) intermolecular interactions, in addition to the well-recognized N–H...O=C and C–H...O=C hydrogen bonds. The presence of such functionalities also allows for the possible existence of C–H...π and π...π interactions. We have synthesized a library of 12 molecules, containing fluorine and trifluoromethyl group, varied over the different positions of the benzene nucleus with respect to PhNHC=OCH<sub>3</sub> (acetamides) and PhC=ONHCH<sub>3</sub> (benzamides). In addition, the unsubstituted compounds, namely acetamide and benzamide, have also been synthesized. The crystal structure of the parent compounds, acetamide<sup>21</sup> and benzamide,<sup>22</sup> are already reported in the literature. These compounds have been found to be the main building block in many biologically active compounds.<sup>23</sup> For example, paracetamol is a well known example amongst these and is widely used as an analgesic and antipyretic.<sup>24</sup> This allows for a comparison of the packing features of fluorinated compounds with non-fluorinated

analogues. It is of interest to note that all the structure determinations have been performed at low temperatures so as to minimize the possibility of dynamic disorder, which is prevalent in fluorine containing substrates.

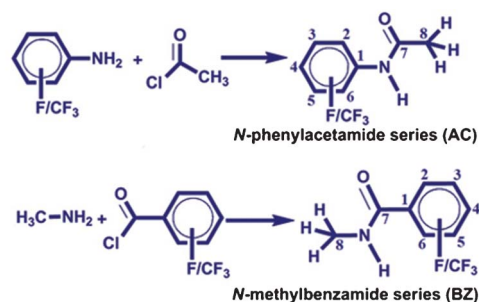
## Experimental section

### Synthesis, characterization and crystal growth

The starting materials, namely aniline along with fluorine and trifluoromethyl substituted anilines, and benzoyl chloride along with fluorine and trifluoromethyl substituted benzoyl chlorides (*ortho*, *meta* and *para*) were purchased from Sigma Aldrich and were used without further purification. The other starting materials, namely methylamine (33% solution in ethanol), acetyl chloride and triethylamine were purchased from Spectrochem Pvt. Ltd. India and were used directly from the bottle. The solvent dichloromethane was dried using calcium hydride and stored over molecular sieves. All the solvents used for crystallization were of analytical grade only.

**(A) Synthesis of N-phenylacetamide.** The compound, aniline or fluorinated/trifluoromethylated derivatives (1.1 equiv.) and triethylamine (1.5 equiv.) were placed in a round bottomed flask containing dry dichloromethane (12.0 ml). This was closed with a septum to ensure a dry atmosphere, using a nitrogen balloon. The reaction set-up was then put over an ice bath and acetylchloride (1 equiv.) was added drop wise into the reaction mixture with constant stirring. The reaction mixture was then allowed to come to RT and the completion of the reaction was monitored with TLC. At the end of the reaction, the reaction mixture was quenched with 5% hydrochloric acid, extracted with dichloromethane, dried using sodium sulphate and finally purified by column chromatography using 10% ethyl acetate in dichloromethane as eluent.

Scheme 1 describes all the molecules synthesized and the method of nomenclature used in this study. Table S1, ESI,† lists the melting points (recorded with DSC and compared with the relevant literature) and the final yields of the product obtained after performing column chromatography.



Sample Code	AC-0	AC-1	AC-2	AC-3	AC-4	AC-5	AC-6
Substitution on Phenyl ring	No substitution	<i>o</i> -F	<i>m</i> -F	<i>p</i> -F	<i>o</i> -CF <sub>3</sub>	<i>m</i> -CF <sub>3</sub>	<i>p</i> -CF <sub>3</sub>
Sample Code	BZ-0	BZ-1	BZ-2	BZ-3	BZ-4	BZ-5	BZ-6
Substitution on Phenyl ring	No substitution	<i>o</i> -F	<i>m</i> -F	<i>p</i> -F	<i>o</i> -CF <sub>3</sub>	<i>m</i> -CF <sub>3</sub>	<i>p</i> -CF <sub>3</sub>

Scheme 1

**(B) Synthesis of *N*-methylbenzamide.** 2 equiv. of cold methylamine (33% solution in ethanol), was added drop wise with constant stirring into the round bottomed flask placed over an ice bath along with 1 equiv. of benzoyl chloride or its fluorinated/trifluoromethylated derivative. The reaction mixture was then stirred at RT for 3 h and the completion of the reaction was monitored with TLC. After completion of the reaction, the reaction mixture was poured into water followed by extraction with diethyl ether and dried using sodium sulphate. The crude product was then purified by column chromatography using 10% ethyl acetate in dichloromethane as eluent.

All the synthesized compounds were characterized by FTIR [Fig. S1(a)–(n), ESI†], <sup>1</sup>H NMR [Fig. S2(a)–(n), ESI†] and <sup>13</sup>C NMR [Fig. S3(a)–(n), ESI†] spectroscopy. Melting points (Table S1, ESI†) were recorded and the DSC traces for all the solid compounds are given in the ESI† [Fig. S4(a)–(n)]. Powder X-ray diffraction (PXRD) data were recorded for all the solid compounds and then compared with the simulated PXRD patterns generated from the crystal coordinates in Mercury 3.0 and the final plots were done in Origin 6.1 [Fig. S5(a)–(n), ESI†].

Single crystals of all the purified solids were grown from different solvents and solvent mixtures (Table 1) at low temperature in a refrigerator. Morphologies ranging from fibrous needles, to thin plates, to blocks to were obtained.

#### Data collection and structure solution and refinement

Single crystal X-ray diffraction data of these compounds (Table 1) were collected on a Bruker AXS SMART APEX CCD diffractometer with X-ray generator operating at 50 kV and 35 mA using graphite monochromated Mo K $\alpha$  ( $\lambda = 0.7107 \text{ \AA}$ ) radiation equipped with Oxford cryosystem 700Plus at 100(2) K. Data reduction and integration were performed by SAINT V7.685A12 (Bruker AXS, 2009) and absorption corrections and scaling was done using SADABS V2008/112 (Bruker AXS). All the crystal structures were solved by direct methods using SIR 92<sup>25</sup> and refined by the full matrix least squares method using SHELXL97<sup>26</sup> present in the program suite WinGX.<sup>27</sup> ORTEP diagrams of all the compounds were generated using ORTEP32<sup>28</sup> and packing diagrams were generated using Mercury software.<sup>29</sup> Geometrical calculations were done using PARST<sup>30</sup> and PLATON.<sup>31</sup> The non-hydrogen atoms are refined anisotropically and the hydrogen atoms bonded to C and N atoms were positioned geometrically and refined using a riding model with distance restraints of N–H = 0.88  $\text{\AA}$ , aromatic C–H = 0.95  $\text{\AA}$ , C(sp<sup>3</sup>)–H = 0.98 and with  $U_{\text{iso}}(\text{H}) = 1.2U_{\text{eq}}(\text{N,C})$ . Table S2, ESI† lists all the geometrically relevant intra and intermolecular interactions in this class of compounds (considered as the sum of the van der Waals radii +0.3  $\text{\AA}$ , angularity >110°). Table S3, ESI† lists all the relevant non-hydrogen atom contacts in the solid state. Amongst all the solved crystal structures, the compounds **AC-5**, **BZ-1** and **BZ-5** were found to be twinned as observed by the presence of high *K*-value in the “shelx.lst” file. In case of **AC-5**, the twin law (a three component non-merohedral twin, the batch scale factors for the minor components are 0.1892 0.0123) were generated by ‘TwinRotMat’ tool in WinGx program suit and the corresponding HKLF5 file were generated by the option tool

‘Make HKLF5’ in WinGX. In the case of **BZ-1**, the inspection of the reflection data by ‘Cell\_Now’ program in APEX-II from Bruker revealed the presence of a three twin component (the contributions of the domain being 0.500, 0.0151, 0.485, respectively). The data-reduction was performed with TWINABS and the refinement was done with BASF scale parameter against HKLF5 reflection file. After the final refinement, in the case of **BZ-1**, the ratio of unique and expected reflections was found to be 1.063. In case of **BZ-5**, the refinement was done with HKLF4 file of the major twin component (the ratio being 0.80 : 0.20), which was separated by the program ‘Cell\_Now’ in APEX-II from Bruker.

#### Crystallographic modeling of disorder

Amongst all the 14 compounds whose crystal structures have been determined accurately using low temperature data, it is observed that in **AC-1** and **BZ-1** (containing two molecules in the asymmetric unit), wherein both the molecules contain a fluorine atom at the *ortho* position, these were found to be disordered at two orientations, the final occupancy ratio being 0.830(2) : 0.170(2) in the case of **AC-1**, and the corresponding values being 0.920(2) : 0.080(2) and 0.921(2) : 0.079(2) for the two independent molecules in the in the asymmetric unit in the case of **BZ-1**. The disorder was analyzed using the PART command in SHELXL97 and were refined for two independent positions, namely A and B (‘A’ depicting the higher occupancy).<sup>32</sup> For the purpose of refinement, the carbon atom positions for A and B in the benzene ring were fixed at same position using the EXYZ command in SHELXL97. Thermal parameters were also constrained to be equal for the atoms at the same position using EADP command in SHELXL97. All the hydrogen atoms were then positioned geometrically and refined using a riding model with  $U_{\text{iso}}(\text{H}) = 1.2U_{\text{eq}}[\text{C}(\text{sp}^2), \text{N}]$  and  $U_{\text{iso}}(\text{H}) = 1.5U_{\text{eq}}[\text{C}(\text{sp}^3)]$ .

#### Theoretical calculations

DFT calculations at the B3LYP/6-31G\*\* were performed using TURBOMOLE<sup>33</sup> with crystallographic coordinates as a starting set (only the major conformer were considered in the case of **AC-1** and **BZ-1**) to obtain the optimized geometry of an isolated molecule. The selected torsion angles obtained from theoretical calculations were then compared with the experimentally obtained values (Table 2). The lattice energies of all the compounds were calculated by PIXELC module in CLP computer program package (version 10.2.2012),<sup>34</sup> the total energy being partitioned into their coulombic, polarization, dispersion and repulsion contributions. These are listed in Table 3. The molecular electron densities were calculated by Gaussian09<sup>35</sup> at the MP2/6-31G\*\* level for the PIXEL energy calculations. For crystal packing and intermolecular energy analysis, the stabilizing molecular pairs have been selected in the crystal related by symmetry operators from *mlc* output file, which is generated after PIXEL energy calculation. The symmetry operator and centroid–centroid distance along with coulombic, polarization, dispersion, repulsion and total interaction energies between the molecular pairs are listed in Table 4. The PIXEL method has been preferred for the quantification of intermolecular interactions, primarily because of the following reasons. (1) It is computationally

Table 1 Crystallographic and refinement data

Data	AC-0	AC-1	AC-2	AC-3 (Form II)	AC-4	AC-5	AC-6
Formula	C <sub>8</sub> H <sub>9</sub> NO	C <sub>8</sub> H <sub>8</sub> NOF	C <sub>8</sub> H <sub>8</sub> NOF	C <sub>8</sub> H <sub>8</sub> NOF	C <sub>9</sub> H <sub>8</sub> NOF <sub>3</sub>	C <sub>9</sub> H <sub>8</sub> NOF <sub>3</sub>	C <sub>9</sub> H <sub>8</sub> NOF <sub>3</sub>
Formula weight	135.16	153.15	153.15	153.15	203.16	203.16	203.16
CCDC no.	907077	907078	907079	907080	907081	907082	907083
Wavelength (Å)	0.71073	0.71073	0.71073	0.71073	0.71073	0.71073	0.71073
Solvent system, temp of crystal growth (°C)	Ether, -20	Ether, -20	DCM + hexane (1 : 1), 5	Ether, -20	Chloroform + hexane (1 : 1), 5	DCM + hexane (1 : 1), 5	DCM, -20
Crystal system	Orthorhombic	Orthorhombic	Orthorhombic	Orthorhombic	Monoclinic	Monoclinic	Orthorhombic
Space group	<i>Pbca</i>	<i>Pbca</i>	<i>Pbca</i>	<i>Pbca</i>	<i>P2<sub>1</sub>/n</i>	<i>P2<sub>1</sub>/c</i>	<i>Pbca</i>
<i>a</i> (Å)	9.4237(4)	10.5091(2)	12.1758(5)	9.4117(4)	4.7762(1)	13.5119(6)	9.6701(5)
<i>b</i> (Å)	7.8685(4)	9.4298(2)	9.4952(5)	7.7523(3)	13.3736(3)	9.7785(4)	9.2755(4)
<i>c</i> (Å)	19.5593(10)	15.1828(5)	12.9071(7)	20.2204(7)	13.9528(3)	6.7775(3)	19.8362(11)
$\alpha$ (°)	90	90	90	90	90	90	90
$\beta$ (°)	90	90	90	90	92.396(1)	99.459(3)	90
$\gamma$ (°)	90	90	90	90	90	90	90
Volume	1450.3(1)	1504.6(1)	1492.2(1)	1475.3(1)	890.46(3)	883.31(7)	1779.2(2)
<i>Z</i>	8	8	8	8	4	4	8
Density (g cm <sup>-3</sup> )	1.238	1.352	1.363	1.379	1.515	1.528	1.517
$\mu$ (mm <sup>-1</sup> )	0.083	0.107	0.108	0.109	0.142	0.143	0.142
<i>F</i> (000)	576	640	640	640	416	416	832
$\theta$ (min, max)	2.08, 27.48	2.68, 27.43	3.15, 27.44	3.55, 27.34	2.11, 27.51	1.53, 25.00	2.05, 24.99
Treatment of hydrogens	Fixed	Fixed	Fixed	Fixed	Fixed	Fixed	Fixed
<i>h</i> <sub>min, max</sub> , <i>k</i> <sub>min, max</sub> , <i>l</i> <sub>min, max</sub>	-12, 11; -10, 8; -25, 24	-13, 13; -12, 12; -19, 14	-15, 15; -8, 12; -12, 16	-11, 11; -9, 9; -26, 22	-6, 6; -15, 17; -18, 16	-16, 15; -11, 11; -6, 8	-11, 11; -11, 10; -23, 12
No. of ref.	7503	6744	6603	6555	7713	1555	7655
No. unique ref./obs. ref.	1659/1400	1693/1515	1681/1317	1632, 1457	2039/1750	1555/1372	1566/1373
No. of parameters	92	111	102	101	128	130	128
<i>R</i> <sub>obs</sub> , <i>R</i> <sub>all</sub>	0.0390, 0.0457	0.0408, 0.0453	0.0381, 0.0532	0.0377, 0.0421	0.0356, 0.0421	0.0394; 0.0457	0.0424, 0.0477
<i>wR</i> <sub>2</sub> (obs), <i>wR</i> <sub>2</sub> (all)	0.1072, 0.1122	0.1103, 0.1144	0.0910, 0.0988	0.0940, 0.0968	0.0868, 0.0903	0.0945, 0.0992	0.1163, 0.1205
$\Delta\rho$ <sub>min, max</sub> (e Å <sup>-3</sup> )	-0.184, 0.190	-0.256, 0.213	-0.237, 0.252	-0.248, 0.217	-0.284, 0.349	-0.363, 0.485	-0.242, 0.468
G. o. F	1.069	1.034	1.080	1.066	1.057	1.089	1.068
Data	BZ-0	BZ-1	BZ-2	BZ-3	BZ-4	BZ-5	BZ-6
Formula	C <sub>8</sub> H <sub>6</sub> NO	C <sub>8</sub> H <sub>8</sub> NOF	C <sub>8</sub> H <sub>8</sub> NOF	C <sub>8</sub> H <sub>8</sub> NOF	C <sub>9</sub> H <sub>8</sub> NOF <sub>3</sub>	C <sub>9</sub> H <sub>8</sub> NOF <sub>3</sub>	C <sub>9</sub> H <sub>8</sub> NOF <sub>3</sub>
Formula weight	135.16	153.15	153.15	153.15	203.16	203.16	203.16
CCDC no.	907084	907085	907086	907087	907088	907089	907090
Wavelength (Å)	0.71073	0.71073	0.71073	0.71073	0.71073	0.71073	0.71073
Solvent system, temp of crystal growth (°C)	DCM, -20	Ether (from solvent extraction), RT	DCM + hexane (1 : 1), 5	DCM + hexane (1 : 1), 5	DCM + hexane (1 : 1), 5	DCM + hexane (1 : 1), 5	DCM + hexane (1 : 1), 5
Crystal system	Orthorhombic	Triclinic	Orthorhombic	Orthorhombic	Monoclinic	Monoclinic	Monoclinic
Space group	<i>Pbca</i>	<i>P1</i>	<i>Pbca</i>	<i>Pbca</i>	<i>P2<sub>1</sub>/c</i>	<i>P2<sub>1</sub>/c</i>	<i>P2<sub>1</sub>/n</i>
<i>a</i> (Å)	9.509(5)	7.490(1)	9.7830(6)	10.9014(5)	11.3520(3)	12.8863(6)	5.0567(3)
<i>b</i> (Å)	9.299(5)	9.776(1)	9.5402(6)	9.9282(4)	8.9766(3)	10.0799(5)	11.6521(5)
<i>c</i> (Å)	16.435(9)	10.358(1)	15.4045(9)	13.3080(6)	8.9705(3)	6.9999(4)	14.6968(7)
$\alpha$ (°)	90	88.856(6)	90	90	90	90	90
$\beta$ (°)	90	85.667(6)	90	90	98.020(2)	103.892(3)	91.565(3)
$\gamma$ (°)	90	75.912(7)	90	90	90	90	90
Volume	1453.3(1)	733.5(2)	1437.7(2)	1440.3(1)	905.17(5)	882.6(1)	865.6(1)
<i>Z</i>	8	4	8	8	4	4	4
Density (g cm <sup>-3</sup> )	1.235	1.387	1.415	1.413	1.491	1.529	1.559
$\mu$ (mm <sup>-1</sup> )	0.082	0.109	0.112	0.111	0.139	0.143	0.146
<i>F</i> (000)	576	320	640	640	416	416	416
$\theta$ (min, max)	2.48, 25.13	1.97, 25.00	9.69, 26.73	3.59, 27.45	1.81, 29.44	1.63, 25.00	2.23, 27.13
Treatment of hydrogens	Fixed	Fixed	Fixed	Fixed	Fixed	Fixed	Fixed
<i>h</i> <sub>min, max</sub> , <i>k</i> <sub>min, max</sub> , <i>l</i> <sub>min, max</sub>	-10, 11; -10, 11; -13, 19	-8, 8; -11, 11; 0, 12	-12, 12; -10, 12; -19, 17	-12, 13; -11, 12; -16, 17	-15, 15; -12, 11; -12, 12	0, 15; -11, 0; -8, 8	-6, 4; -14, 14; -18, 18
No. of ref.	5308	2740	7433	6468	17 386	1549	6844
No. unique ref./obs. ref.	1286, 873	2740/2409	1425/1200	1633/1395	2508/2136	1549/1412	1904/1543
No. of parameters	93	212	101	101	128	128	128
<i>R</i> <sub>obs</sub> , <i>R</i> <sub>all</sub>	0.0452, 0.0702	0.0501, 0.0544	0.0410, 0.0496	0.0359, 0.0433	0.0359, 0.0435	0.0481, 0.0525	0.0406, 0.0511
<i>wR</i> <sub>2</sub> (obs), <i>wR</i> <sub>2</sub> (all)	0.1125, 0.1502	0.1562, 0.1600	0.1248, 0.1474	0.0924, 0.0972	0.0901, 0.0943	0.1340, 0.1377	0.1042, 0.1105
$\Delta\rho$ <sub>min, max</sub> (e Å <sup>-3</sup> )	-0.213, 0.201	-0.281, 0.438	-0.205, 0.262	-0.240, 0.229	-0.230, 0.357	-0.296, 0.298	-0.298, 0.302
G. o. F	1.109	1.128	1.127	1.087	1.061	1.135	1.103

less demanding.<sup>34</sup> (2) The total interaction energy is partitioned into the corresponding coulombic, polarization, dispersion, and repulsion contribution. This facilitates a better

understanding of the nature of intermolecular interactions contributing towards the crystal packing.<sup>3a,c,e,g</sup> The results obtained from PIXEL calculation were found to be comparable

**Table 2** Selected torsion angles (°). Only major conformers were considered for disordered molecules. Values in *italics* are obtained from theoretical B3LYP/6-31G\*\* calculation

Compound Code	<i>N</i> -Phenylacetamide series	
	C7–N1–C1–C6	C1–N1–C7–C8
<b>AC-0</b>	161.8(1)	176.0(1)
	<i>171.11</i>	<i>178.38</i>
<b>AC-1</b>	145.8(1)	177.9(1)
	<i>179.97</i>	<i>178.99</i>
<b>AC-2</b>	168.5(1)	174.9(1)
	<i>179.64</i>	<i>178.22</i>
<b>AC-3 Form I/Form II</b>	161.7(1)/177.6(1)	176.3(1)/178.5(1)
	<i>179.77</i>	<i>179.77</i>
<b>AC-4</b>	128.4(1)	173.3(1)
	<i>173.14</i>	<i>179.16</i>
<b>AC-5</b>	178.7(2)	178.3(2)
	<i>179.90</i>	<i>179.94</i>
<b>AC-6</b>	172.0(2)	179.8(2)
	<i>179.43</i>	<i>179.47</i>

	<i>N</i> -Methylbenzamide series	
	C2–C1–C7–N1	C8–N1–C7–C1
<b>BZ-0</b>	167.1(2)	179.2(2)
	<i>158.00</i>	<i>176.06</i>
<b>BZ-1</b>	157.26(10)/154.32(9) <sup>a</sup>	175.65(9)/176.84(9) <sup>a</sup>
	<i>162.48/170.60</i>	<i>177.35/177.37</i>
<b>BZ-2</b>	170.8(1)	178.1(1)
	<i>158.87</i>	<i>176.52</i>
<b>BZ-3</b>	162.6(1)	179.5(1)
	<i>160.24</i>	<i>177.26</i>
<b>BZ-4</b>	105.3(1)	179.0(1)
	<i>134.52</i>	<i>178.41</i>
<b>BZ-5</b>	176.6(2)	177.8(2)
	<i>159.10</i>	<i>176.71</i>
<b>BZ-6</b>	146.6(1)	178.5(1)
	<i>158.84</i>	<i>176.28</i>

<sup>a</sup> Equivalent torsion angle of the second molecule in the asymmetric unit.

with high level MP2 and DFT-D quantum mechanical calculations, the latter two being more computationally demanding.<sup>3b,c,34</sup> It is obvious that the molecular pair energy calculated in this way may or may not correspond to the energy minima, as molecules in the solid state are subjected to constant electric fields.<sup>3e</sup> Therefore for the sake of comparison, the interaction energy of the selected isolated molecular pairs at the crystal geometry have also been calculated using TURBOMOLE at DFT-D3/B97-D level of calculation with the aug-cc-pVTZ basis set. The final interaction energies are listed along with the PIXEL energies in Table 4. The new DFT-D3 method is moderately computationally demanding and is applicable to all the elements of the periodic table. The energy estimates derived for non-covalent interactions and van der Waals complexes are accurate. In particular, the estimation of the dispersion energy has been found to be more accurate than the values derived from old DFT-D or DFT-D2 methods.<sup>36</sup> The DFT-D3 method were also found to work better with B97-D functional than previously employed DFT-D or DFT-D2 methods.<sup>36a,37</sup> The larger basis set (aug-cc-pVTZ) for DFT-D3/B97-D level calculation is so chosen that it minimizes the

**Table 3** Lattice energy calculations using CLP (in kcal mol<sup>-1</sup>)

Comp. Code	$E_{\text{Coul}}$	$E_{\text{Pol}}$	$E_{\text{Disp}}$	$E_{\text{Rep}}$	$E_{\text{Tot}}^a$
1 <b>AC-0</b>	-14.1	-5.5	-22.4	19.0	-23.1
2 <b>AC-1</b>	-15.3	-6.2	-21.5	20.9	-22.1
3 <b>AC-2</b>	-16.1	-6.9	-22.0	21.8	-23.2
4a <b>AC-3 Form I [SAZLEL]</b>	-11.5	-4.6	-19.0	16.5	-18.6
4b <b>AC-3 Form II</b>	-15.2	-6.3	-22.6	20.5	-23.6
5 <b>AC-4</b>	-14.6	-5.8	-22.7	19.7	-23.4
6 <b>AC-5</b>	-13.6	-5.9	-23.7	21.1	-22.2
7 <b>AC-6</b>	-14.3	-5.6	-21.7	18.1	-23.5
8 <b>BZ-0</b>	-15.6	-7.0	-24.2	23.9	-22.9
9 <b>BZ-1</b>	-10.5	-4.4	-22.1	16.9	-20.1
10 <b>BZ-2</b>	-15.3	-6.6	-24.0	22.5	-23.4
11 <b>BZ-3</b>	-14.1	-6.2	-23.6	21.1	-22.8
12 <b>BZ-4</b>	-15.0	-5.8	-21.8	19.3	-23.2
13 <b>BZ-5</b>	-13.7	-6.2	-23.6	21.2	-22.2
14 <b>BZ-6</b>	-14.1	-5.0	-23.8	18.7	-24.2

<sup>a</sup> Sublimation energies reported in the literature are 23.9 kcal mol<sup>-1</sup> and 24.1 kcal mol<sup>-1</sup> for *N*-phenylacetamide and *N*-methylbenzamide respectively.<sup>39</sup>

requirement for the calculation of basis set superposition error.<sup>36b,37</sup> For the sake of comparison, the energies obtained from PIXEL calculations with high level theoretical calculations, we have computed the BSSE corrected energies, using MP2 and DFT-D2 methods of calculation for only two molecules namely, **AC-1** and **BZ-5** (Table S5, ESI†). The interaction energy of the molecular pairs ( $\Delta E_{\text{dimer}}$ ) were calculated using the formula  $\Delta E_{\text{dimer}} = [E_{\text{dimer}} - (2 \times E_{\text{monomer}})]$ . The positions of hydrogen atoms were moved to neutron values (1.08 Å for C–H and 1.00 Å for N–H) before the calculation. It is to be noted that compound **AC-3** exists in two forms (hereafter referred to Form I and II). The crystal structure of Form I is already reported in the literature.<sup>38</sup>

## Results and discussion

Fig. S6(a)–(n), ESI† show the ORTEP for all the compounds.

### 1. *N*-Phenylacetamide (**AC-0**)

The parent compound *N*-phenylacetamide (**AC-0**) crystallizes in a centrosymmetric orthorhombic space group *Pbca* with  $Z = 8$  [Fig. S5(a), ESI†]. The packing of molecules in the crystal structure depicts the formation of a molecular chain *via* strong N–H⋯O hydrogen bonds along with weak C–H⋯O hydrogen bonds which indicates the existence of a stabilizing molecular motif 1 (−8.8 kcal mol<sup>-1</sup>) in the crystal structure, having a major coulombic contribution [Table 4, Fig. 1(a)]. The molecular chains are then interlinked *via* weak C8–H8A⋯O1 and C3–H3⋯π hydrogen bonds [Fig. 1(b)], these having a contribution of −5.0 kcal mol<sup>-1</sup> in stabilization, the dispersion contribution imparting the maximum stabilization [Table 4, motif 3, Fig. 1(a)]. The second most stabilized molecular pair found in the crystal packing are the stacked dimers [3.576 Å, Fig. 1(a)], these contributing −6.9 kcal mol<sup>-1</sup> to the crystal stabilization, the dispersion contribution again being a major component [Table 4, Fig. 1(c)]. The interaction energy of the packing motif 1 in the crystal was found to be

**Table 4** PIXEL interaction energies (I.E.) (kcal mol<sup>-1</sup>) between molecular pairs related by a symmetry operation and the associated intermolecular interactions in the crystal

Serial No.	Symmetry code	Centroid-centroid distance (Å)	$E_{\text{Coul}}$	$E_{\text{Pol}}$	$E_{\text{Disp}}$	$E_{\text{Rep}}$	$E_{\text{Tot}}$	DFT-D3/B97-D aug-cc-pVTZ	Involved interactions
<b>AC-0 (Pbca)</b>									
1	$x - 1/2, -y + 1/2, -z + 1$	5.922	-9.3	-3.5	-5.5	9.5	-8.8	-8.75	N1-H1...O1, C6-H6...O1, C8-H8B...O1
2	$-x + 1, -y, -z + 1$	4.254	-3.2	-0.8	-7.4	4.5	-6.9	-9.23	Molecular stacking
3	$-x + 3/2, y + 1/2, z$	4.735	-2.6	-1.0	-5.3	3.9	-5.0	-6.38	C8-H8A...O1, C3-H3...Cg1
<b>AC-1 (Pbca)</b>									
1	$-x + 3/2, y - 1/2, z$	6.334	-11.9	-4.5	-5.2	12.9	-8.6	-8.50	N1-H1...O1, C8-H8B...O1, C8-H8C...F1A
2	$-x + 2, -y + 2, -z + 1$	4.274	-0.4	-0.5	-6.7	3.7	-3.9	-5.76	Molecular stacking
3	$x - 1/2, y, -z + 3/2$	6.292	-0.5	-0.5	-4.4	2.3	-3.2	-3.45	C5A-H5A...F1A, C4A-H4A...F1A
4	$-x + 2, y + 1/2, -z + 3/2$	5.938	-0.7	-0.5	-2.2	1.1	-2.2	-2.56	C5A-H5A...O1
5	$x + 1/2, -y + 3/2, -z + 1$	7.965	-0.5	-0.3	-2.0	0.8	-2.1	-2.33	C3A-H3A...O1
<b>AC-2 (Pbca)</b>									
1	$-x + 3/2, y - 1/2, z$	6.744	-11.3	-4.4	-5.2	12.0	-8.9	-8.41	N1-H1...O1, C8-H8B...O1
2	$-x + 1, -y, -z + 1$	3.446	-3.4	-1.0	-9.2	7.1	-6.7	-9.45	Molecular stacking
3	$-x + 1, y - 1/2, -z + 3/2$	5.910	-1.0	-0.6	-3.5	2.1	-3.1	-3.41	C6-H6...F1, C5-H5...O1
4	$x - 1/2, y, -z + 3/2$	6.912	0.1	-0.6	-3.7	2.6	-1.7	-2.49	C4-H4...N1/ $\pi$
5	$-x + 1/2, y - 1/2, z$	8.780	-0.3	-0.2	-1.4	0.7	-1.1	-0.93	C5-H5...F1
6	$x + 1/2, -y + 1/2, -z + 1$	8.198	-0.1	-0.2	-0.8	0.2	-0.9	-1.00	C8-H8A...F1
<b>AC-3-Form I (Cc)</b>									
1	$x, -y + 1, z + 1/2$	6.147	-10.5	-3.9	-4.5	10.8	-8.0	-8.08	N1-H1...O1, C6-H6...O1, C8-H8B...O1
2	$x + 1, y, z$	4.731	0.2	-0.5	-5.7	2.4	-3.7	-5.32	Molecular stacking
3	$x - 1/2, -y + 1/2, z + 1/2$	7.223	-0.9	-0.2	-2.0	0.8	-2.3	-2.44	C6-H6...F1
4	$x + 1/2, -y + 1/2, z + 1/2$	7.063	-0.5	-0.2	-1.8	0.9	-1.6	-1.92	C5-H5...Cg1
5	$x + 1/2, y - 1/2, z$	8.855	0.0	-0.2	-1.3	0.5	-0.9	-1.27	C8-H8A...F1
6	$x + 3/2, y - 1/2, z$	11.098	-0.4	-0.1	-0.7	0.5	-0.7	-0.72	C8-H8C...F1
<b>AC-3-Form II (Pbca)</b>									
1	$x + 1/2, -y + 3/2, -z$	6.578	-9.7	-3.8	-5.6	10.2	-8.8	-8.74	N1-H1...O1, C6-H6...O1
2	$-x + 1, -y + 2, -z$	5.008	-3.0	-0.9	-7.4	4.7	-6.6	-8.99	Molecular stacking
3	$-x + 1/2, y - 1/2, z$	4.562	-3.0	-1.2	-5.9	4.9	-5.2	-6.78	C8-H8A...O1, C3-H3...Cg1
4	$-x + 1, y - 1/2, -z + 1/2$	7.526	-1.2	-0.3	-2.2	1.6	-2.2	-2.02	C6-H6...F1, C5-H5...F1
5	$x, -y + 3/2, z - 1/2$	10.328	-0.1	-0.1	-1.0	0.5	-0.8	-0.73	C8-H8A...F1
<b>AC-4 (P2<sub>1</sub>/n)</b>									
1	$x - 1, y, z$	4.776	-9.7	-3.7	-6.7	10.9	-9.1	-9.30	N1-H1...O1, C8-H8B...O1, C9-F3...O1-C7, C9-F2...F3-C9
2	$-x + 1, -y + 2, -z$	7.634	-3.3	-1.4	-4.4	3.2	-5.9	-6.20	C3-H3...O1
3	$-x, -y + 2, -z$	6.114	-0.4	-0.6	-6.9	4.3	-3.6	-4.62	Molecular stacking
4	$x + 1/2, -y + 3/2, z + 1/2$	7.335	-1.3	-0.5	-2.3	1.2	-2.9	-3.25	C8-H8A...F1, H8A...H5
5	$x + 1/2, -y + 3/2, z - 1/2$	7.523	-0.4	-0.6	-4.2	2.6	-2.7	-2.50	C3-H3...F2, C4-H4...F2
6	$-x - 1/2, y + 1/2, -z + 1/2$	8.819	-0.5	-0.1	-1.3	0.6	-1.4	-1.22	C8-H8C...F3
7	$-x + 1/2, y + 1/2, -z + 1/2$	8.548	-0.3	-0.2	-1.0	0.6	-0.9	-0.90	C8-H8C...F1
<b>AC-5 (P2<sub>1</sub>/c)</b>									
1	$-x, y - 1/2, -z + 1/2$	7.976	-10.1	-4.0	-6.3	11.6	-8.7	-8.25	N1-H1...O1, C8-H8B...O1
2	$-x, -y + 2, -z$	6.575	-2.4	-0.8	-4.5	1.9	-5.8	-7.05	C=O...O=C
3	$-x, -y + 2, -z + 1$	7.812	-3.3	-0.7	-3.5	1.8	-5.6	-6.70	C8-H8A...O1, C=O...C=O
4	$x, -y + 3/2, z - 1/2$	5.184	-2.2	-1.0	-8.6	6.4	-5.3	-7.92	Cg1...Cg1
5	$-x + 1, -y + 2, -z$	8.410	-0.7	-0.1	-1.3	0.6	-1.5	-1.55	C4-H4...F3, C9-F3...F3-C9
6	$-x + 1, y - 1/2, -z + 1/2$	8.721	-0.3	-0.2	-1.6	0.5	-1.5	-1.36	C4-H4...F2
7	$-x + 1, -y + 2, -z + 1$	7.643	-0.5	-0.1	-1.3	0.4	-1.5	-1.61	C9-F2...F2-C9
8	$x, -y + 5/2, z + 1/2$	6.766	1.0	-0.1	-0.8	0.1	0.2	-0.23	C9-F2...F3-C9
<b>AC-6 (Pbca)</b>									
1	$x - 1/2, y, -z + 1/2$	7.756	-10.1	-3.8	-4.3	10.2	-8.1	-7.86	N1-H1...O1, C6-H6...O1, C8-H8C...O1
2	$-x + 3/2, y + 1/2, z$	4.666	-1.1	-0.7	-7.3	3.6	-5.5	-7.02	Stacking moiety, C...C, C-F...C
3	$-x + 1, -y + 2, -z + 1$	8.315	-1.5	-0.3	-1.8	1.8	-1.8	-1.91	C5-H5...F3, C9-F3...F3-C9
4	$x, -y + 3/2, z - 1/2$	9.927	-0.6	-0.1	-1.1	0.5	-1.4	-1.63	C8-H8B...F1
5	$-x + 2, -y + 2, -z + 1$	7.693	-0.5	-0.2	-1.7	1.5	-1.0	-1.07	C3-H3...F1, C9-F1...F1-C9
<b>BZ-0 (Pbca)</b>									
1	$x + 1/2, -y + 1/2, -z + 1$	5.817	-11.3	-4.6	-6.7	13.8	-8.8	-8.74	N1-H1...O1, C6-H6...O1
2	$-x + 1, -y, -z + 1$	3.731	-2.7	-1.2	-8.4	6.3	-6.0	-7.93	Molecular stacking
3	$-x + 1/2, y + 1/2, z$	5.187	-1.8	-0.8	-5.0	3.4	-4.2	-5.20	C8-H8A...O1
<b>BZ-1 (P<math>\bar{1}</math>, Z' = 2) A...A</b>									

Table 4 (Continued)

Serial No.	Symmetry code	Centroid-centroid distance (Å)	$E_{\text{Coul}}$	$E_{\text{Pol}}$	$E_{\text{Disp}}$	$E_{\text{Rep}}$	$E_{\text{Tot}}$	DFT-D3/B97-D aug-cc-pVTZ	Involved interactions
1	$-x + 2, -y + 1, -z + 1$	3.795	-1.8	-0.8	-6.7	4.1	-5.2	-7.30	Molecular stacking
2	$-x + 1, -y + 1, -z + 1$	4.046	-0.5	-0.5	-7.8	4.9	-3.9	-6.11	Molecular stacking
<b>A<math>\cdots</math>B/B<math>\cdots</math>A</b>									
3	$x, y + 1, z$	6.245	-6.6	-2.5	-4.4	6.9	-6.6	-5.84	N2-H2 $\cdots$ O1, C16-H16B $\cdots$ O1, C8-H8C $\cdots$ F2A
4	$x, y, z$	6.324	-6.2	-2.3	-4.4	6.7	-6.2	-5.61	N1-H1 $\cdots$ O2, C8-H8B $\cdots$ O2, C16-H16A $\cdots$ F1A
5	$-x + 1, -y + 1, -z$	7.973	-2.0	-0.8	-2.2	1.9	-3.1	-3.15	C11A-H11A $\cdots$ O1
6	$-x + 1, -y + 1, -z + 1$	7.537	-1.5	-0.8	-2.4	1.7	-3.0	-3.04	C3A-H3A $\cdots$ O2
7	$-x + 2, -y, -z + 1$	7.229	-1.0	-0.5	-3.3	2.0	-2.8	-2.42	C4A-H4A $\cdots$ F2A, C16-H16B $\cdots$ F1A
8	$-x + 2, -y, -z$	7.165	-0.8	-0.4	-2.9	1.5	-2.6	-2.33	C8-H8B $\cdots$ F2A, C13A-H13A $\cdots$ F1A, C12A-H12A $\cdots$ F1A
<b>B<math>\cdots</math>B</b>									
9	$-x + 2, -y, -z$	3.720	-1.3	-0.8	-6.7	4.2	-4.7	-7.06	Molecular stacking
10	$-x + 1, -y, -z$	4.268	-0.8	-0.6	-7.7	5.2	-3.9	-6.33	Molecular stacking
<b>BZ-2 (Pbca)</b>									
1	$x + 1/2, -y + 3/2, -z + 1$	6.563	-10.3	-4.0	-6.2	11.6	-9.0	-8.53	N1-H1 $\cdots$ O1, C6-H6 $\cdots$ O1
2	$-x + 1, -y + 2, -z + 1$	3.714	-3.6	-1.6	-9.4	8.6	-6.1	-8.61	Molecular stacking
3	$-x + 1/2, y - 1/2, z$	5.516	-1.4	-0.7	-4.3	2.6	-3.7	-4.26	C8-H8A $\cdots$ O1, C-F $\cdots$ $\pi$
4	$-x + 1, y + 1/2, -z + 3/2$	7.208	-1.2	-0.4	-2.3	1.2	-2.7	-2.82	C5-H5 $\cdots$ F1, C4-H4 $\cdots$ C
5	$x + 1/2, y, -z + 3/2$	6.973	-0.7	-0.4	-2.7	1.9	-2.0	-1.99	C4-H4 $\cdots$ F1, C5-H5 $\cdots$ F1
6	$-x + 1/2, -y + 2, z + 1/2$	8.296	-0.6	-0.1	-0.5	0.1	-1.2	-1.45	C8-H8C $\cdots$ F1
<b>BZ-3 (Pbca)</b>									
1	$-x + 1/2, y + 1/2, z$	6.795	-9.6	-3.9	-5.9	10.8	-8.7	-8.15	N1-H1 $\cdots$ O1, C6-H6 $\cdots$ O1
2	$-x + 1, -y + 2, -z + 1$	3.552	-1.2	-0.8	-8.7	6.0	-4.7	-7.12	Molecular stacking, C8-H8C $\cdots$ F1
3	$x - 1/2, y, -z + 1/2$	6.365	-0.9	-0.6	-5.1	3.8	-2.7	-3.69	C6-H6 $\cdots$ F1, C8-H8A $\cdots$ Cg1
4	$x + 1/2, -y + 3/2, -z + 1$	7.648	-0.8	-0.5	-1.9	1.1	-2.1	-2.50	C3-H3 $\cdots$ O1
5	$-x + 1, y + 1/2, -z + 1/2$	6.008	-0.3	-0.4	-1.9	0.5	-2.0	-2.42	C5-H5 $\cdots$ O1
6	$-x + 3/2, y - 1/2, z$	7.990	-0.5	-0.3	-2.0	1.1	-1.6	-1.43	C3-H3 $\cdots$ F1, C2-H2 $\cdots$ F1
7	$x - 1, y, z$	10.901	-0.6	-0.1	-0.7	0.4	-1.0	-1.01	C8-H8B $\cdots$ F1
<b>BZ-4 (P2<sub>1</sub>/c)</b>									
1	$x, -y + 3/2, z - 1/2$	5.777	-8.8	-3.4	-6.2	10.2	-8.3	-8.92	N1-H1 $\cdots$ O1, C8-H8B $\cdots$ O1, C8-H8C $\cdots$ Cg1, C9-F2 $\cdots$ F3-C9
2	$-x + 1, -y + 2, -z + 2$	7.185	-5.3	-1.6	-3.9	3.9	-7.0	-7.43	C2-H2 $\cdots$ O1
3	$x, -y + 5/2, z + 1/2$	6.970	-1.8	-0.9	-3.5	2.3	-3.8	-4.42	C4-H4 $\cdots$ O1, C4-H4 $\cdots$ C
4	$-x, -y + 2, -z + 1$	6.559	-1.1	-0.2	-2.5	1.1	-2.7	-2.56	C5-H5 $\cdots$ F3, C4-H4 $\cdots$ Cg1
5	$-x, y + 1/2, -z + 3/2$	6.523	-1.2	-0.3	-2.4	1.2	-2.6	-2.49	C5-H5 $\cdots$ F3, C9-F1 $\cdots$ F2-C9
<b>BZ-5 (P2<sub>1</sub>/c)</b>									
1	$-x, y - 1/2, -z + 1/2$	7.851	-10.2	-4.3	-6.7	12.5	-8.7	-8.24	N1-H1 $\cdots$ O1, C6-H6 $\cdots$ O1
2	$x, -y + 3/2, z + 1/2$	5.134	-2.1	-0.7	-7.3	4.5	-5.6	-7.72	C $\cdots$ C, stacking
3	$-x, -y + 2, -z$	6.209	-2.2	-1.0	-5.5	3.2	-5.6	-6.50	C=O $\cdots$ C=O
4	$-x, -y + 2, -z + 1$	7.856	-2.2	-0.7	-3.6	1.9	-4.6	-5.87	C8-H8A $\cdots$ O1
5	$-x + 1, -y + 2, -z + 1$	7.147	-0.5	-0.1	-2.0	0.6	-2.0	-1.80	C9-F2 $\cdots$ F3-C9, C9-F3 $\cdots$ F3-C9
6	$-x + 1, y - 1/2, -z + 1/2$	8.523	-0.6	-0.3	-1.9	1.1	-1.6	-1.45	C5-H5 $\cdots$ F3, C4-H4 $\cdots$ F2
7	$-x + 1, -y + 2, -z$	8.439	-0.2	-0.1	-1.1	0.3	-1.1	-0.93	C9-F1 $\cdots$ F3-C9
<b>BZ-6 (P2<sub>1</sub>/n)</b>									
1	$x + 1, y, z$	5.057	-9.3	-3.1	-6.4	9.2	-9.6	-9.63	N1-H1 $\cdots$ O1, C3-H3 $\cdots$ F1, C9-F1 $\cdots$ F2-C9
2	$-x, -y + 1, -z + 2$	7.003	-4.3	-1.2	-6.1	4.0	-7.7	-9.45	C6-H6 $\cdots$ O1, C8-H8A $\cdots$ Cg1
3	$-x - 1/2, y + 1/2, -z + 3/2$	7.866	-1.6	-0.7	-2.8	1.8	-3.3	-3.37	C3-H3 $\cdots$ O1, C2-H2 $\cdots$ F2
4	$-x + 1/2, y + 1/2, -z + 3/2$	7.003	-0.4	-0.3	-4.2	2.1	-2.8	-3.11	C2-H2 $\cdots$ F1, stacking
5	$-x + 1, -y + 1, -z + 2$	7.729	0.5	-1.0	-5.3	3.0	-2.8	-2.79	Dimeric moiety, C6-H6 $\cdots$ N1-C8
6	$-x + 1, -y, -z + 2$	7.798	-1.6	-0.4	-2.2	2.0	-2.3	-2.11	C5-H5 $\cdots$ F3
7	$x, y + 1, z$	11.652	-0.5	-0.1	-1.5	0.7	-1.4	-1.15	C8-H8C $\cdots$ F2, CH <sub>3</sub> $\cdots$ CF <sub>3</sub> - moiety

similar to that of the isolated dimer, while that of the stacked motif 2 has an extra stabilization of 2.3 kcal mol<sup>-1</sup> in the gas phase when compared with the solid state (Table 4).

## 2. N-(2-Fluorophenyl)acetamide (AC-1)

The compound AC-1 crystallizes in an orthorhombic centrosymmetric space group *Pbca* with  $Z = 8$  [Fig. S5(b), ESI†]. The molecule exhibits positional disorder of the fluorine atom at two sites, the final occupancy ratio refining to a value of

0.830(2) : 0.170(2). Strong N-H $\cdots$ O=C H-bonds along with weak C(sp<sup>3</sup>)-H $\cdots$ O=C and C(sp<sup>3</sup>)-H $\cdots$ F-C(sp<sup>2</sup>) H-bonds (motif 1, -8.6 kcal mol<sup>-1</sup>) are involved in the formation of molecular chains, with the utilization of the *b*-glide perpendicular to the crystallographic *a* axis [Fig. 2(b)]. The chains thus formed are interconnected with weak C(sp<sup>2</sup>)-H $\cdots$ O=C [motif 4 and motif 5, both having similar interaction energy (-2.2 and -2.1 kcal mol<sup>-1</sup>, respectively) in the crystal, Table 4] in addition to molecular stacking (Table 4, motif 2, -3.9 kcal mol<sup>-1</sup>)

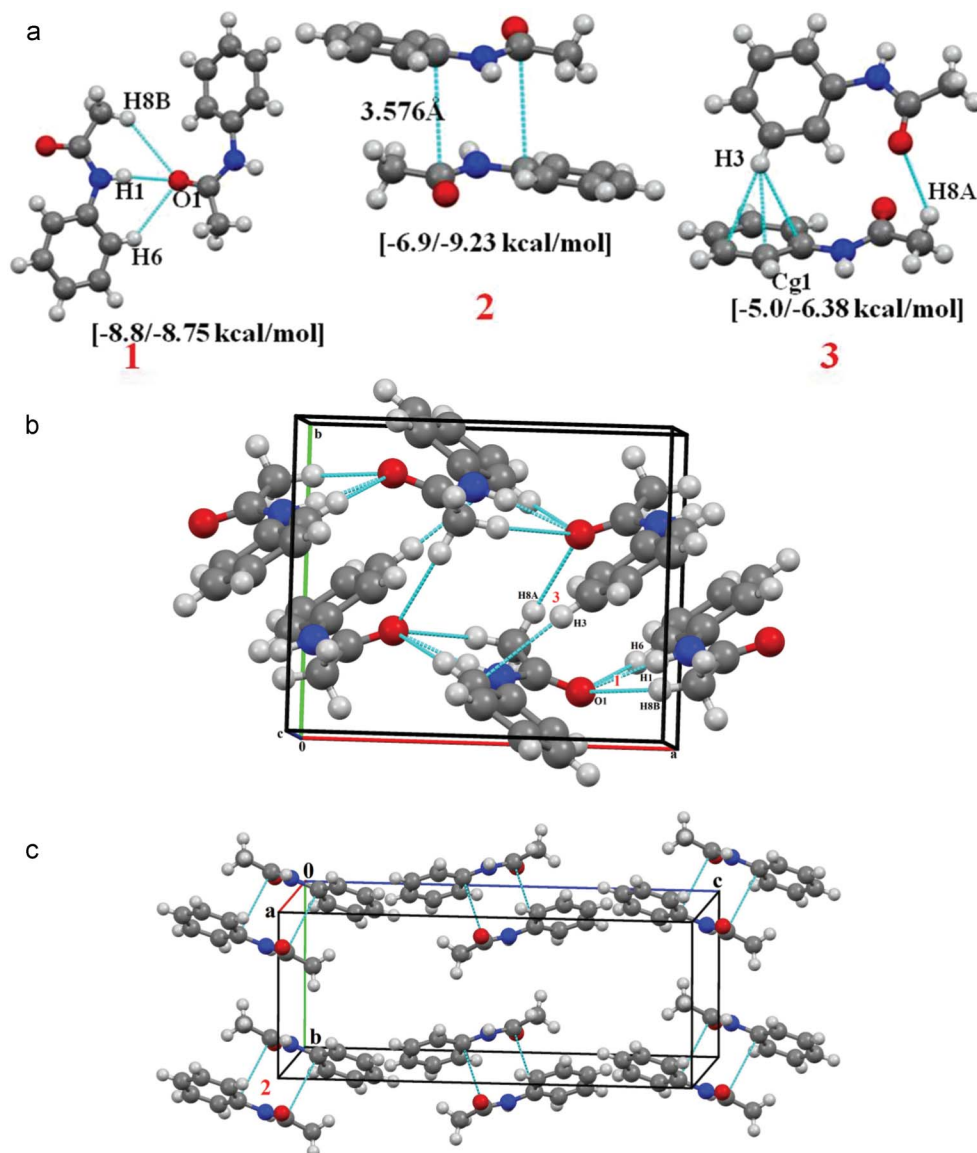


**Fig. 1** (a) Selected molecular pairs from Table 4 (denoted as red numbers) depicting inter molecular contacts in **AC-0**. The values in brackets denote interaction energies from PIXEL and DFT-D3 calculations. (b) Packing of molecules down the *ab* plane in **AC-0** via N-H $\cdots$ O, C-H $\cdots$ O and C-H $\cdots$  $\pi$  hydrogen bonds in **AC-0**. (c) Packing of molecular dimers down the *bc* plane in **AC-0**.

[Fig. 2(b)], which is a primary building block in the crystalline structure. The third most stabilizing “molecular pair” found to link *via* bifurcated C(sp<sup>2</sup>)-H $\cdots$ F-C(sp<sup>2</sup>) [utilizing the *a*-glide, Fig. 2(c), motif 3] with I.E. = -3.2 kcal mol<sup>-1</sup>. It is of interest to note that the major contribution comes from dispersion (Table 4) in contrast to coulombic and polarization components, which for motif 3 are small. It is noteworthy that PIXEL interaction energies of all molecular pairs are found to be similar to that of the isolated pair except 2 (behaves 1.9 kcal more stable as isolated pair than in crystal environment) (Table 4).

### 3. *N*-(3-Fluorophenyl)acetamide (**AC-2**)

The compound **AC-2** crystallizes in the centrosymmetric orthorhombic space group *Pbca* with *Z* = 8, with a character-

istic intramolecular C-H $\cdots$ O=C hydrogen bond [Fig. S5(c), ESI†]. The molecules are packed with the involvement of strong N-H $\cdots$ O=C hydrogen bonds along with C(sp<sup>3</sup>)-H $\cdots$ O=C generating a molecular chain with the utilization of *b*-glide perpendicular to crystallographic *a*-axis [motif 1, I.E. = -8.9 kcal mol<sup>-1</sup>, Fig. 3(b)]. The chains thus formed are interconnected with weak C(sp<sup>2</sup>)-H $\cdots$ F(sp<sup>2</sup>) (involves H5 with F1, motif 5, I.E. = -1.1 kcal mol<sup>-1</sup>) hydrogen bonds and generate a molecular sheet down the *ab* plane. The second most stable molecular pair in the crystal structure, formed *via* molecular stacking, has a contribution of -6.7 (motif 2) to the stabilization of the crystal packing. Adjacent stacks are connected *via* weak C(sp<sup>2</sup>)-H5 $\cdots$ O=C and C(sp<sup>2</sup>)-H6 $\cdots$ F1-C(sp<sup>2</sup>) [motif 3, I.E. = -3.1 kcal mol<sup>-1</sup>, the major contribution being the dispersion energy, Table 4, Fig. 3(c)] intermolecular

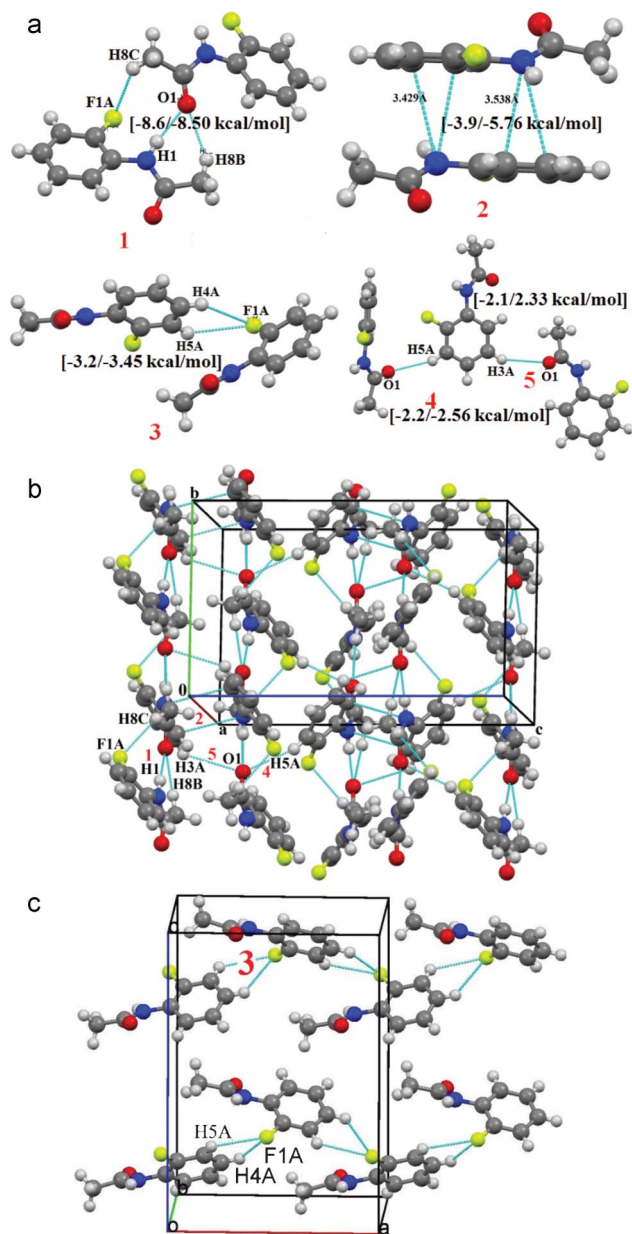


**Fig. 2** (a) The molecular pairs (red numbers denoting as in Table 4) along with their interaction energy from PIXEL and DFT-D3 (Table 4) calculations in **AC-1**. (b) Packing view down the  $bc$ -plane in **AC-1**. The number in red denotes corresponding molecular pairs in Table 4. (c) Packing view down the  $ac$  plane, showing formation of parallel molecular chains *via* weak  $C(sp^2)\text{-H}\cdots\text{F}$  hydrogen bonds along  $a$ -axis in **AC-1**.

H-bonds. The decrease in the interaction energy of the molecular pair 2, from  $-9.45 \text{ kcal mol}^{-1}$  to  $-6.7 \text{ kcal mol}^{-1}$  (in the isolated pair), provides an excellent example to explore the co-operative nature of weak interactions in the crystal environment [depicted in the blue circle in Fig. 3(c), where motifs 2 and 3 are present together]. The packing in the crystal also involves the formation of molecular chains with  $C(sp^3)\text{-H}\cdots\text{F}(sp^2)$  (involving H8A), contributing  $-0.9 \text{ kcal mol}^{-1}$  (mainly dispersion contribution, Table 4, motif 6), with  $2_1$ -screw along  $a$ -axis. The molecular chains are then intercon-

nected with more stabilized motif 4 (I.E. =  $-1.7 \text{ kcal mol}^{-1}$ ) [Fig. 3(d)].

It should also be noted that the incorporation of a fluorine atom over the phenyl ring of the parent compound, **AC-0**, at either *ortho* (**AC-1**) or *meta* (**AC-2**) position does not change the total lattice energy but increases the possibility of formation of different molecular motifs [motif 3 in **AC-1**, motifs 3, 5 and 6 in **AC-2**, Fig. 2(a) and 3(a)] which can contribute to the stabilization of the crystal structure. This results in the alteration in the crystal packing from the parent compound while displaying similar packing to each other.

#### 4. *N*-(3-Fluorophenyl)acetamide (**AC-3**)

The crystal structure of the compound *N*-(3-fluorophenyl)acetamide (**AC-3**) was already reported in the literature<sup>37</sup> and retrieved from the CCDC (Ref code SAZLEL), hereby referred as Form I. Crystals of this compound were obtained by slow evaporation from ethyl acetate solution, the crystals exhibiting prism-like morphology. The compound crystallized in the non-centrosymmetric monoclinic space group  $Cc$  with  $Z = 4$  molecules in the unit cell, the cell parameter being:  $a = 4.731(2) \text{ \AA}$ ,  $b = 17.067(5) \text{ \AA}$ ,  $c = 9.634(3) \text{ \AA}$ ,  $\beta = 92.871(5)^\circ$ ,  $V = 776.8 \text{ \AA}^3$ . Various attempts to get single crystals of the above-mentioned Form I were unsuccessful. On the contrary, the obtained crystals [Fig. 4(a)] from ether solution at low temperature displayed plate-like morphology. The crystal structure of the new form, referred to as Form II, crystallized in the centrosymmetric orthorhombic  $Pbca$  space group with  $Z = 8$  molecules in the unit cell [Fig. S5(d), ESI<sup>†</sup>], the lattice parameters for the new form being  $a = 9.4117(4) \text{ \AA}$ ,  $b = 7.7523(3) \text{ \AA}$ ,  $c = 20.2204(7) \text{ \AA}$ ,  $V = 1475.3(1) \text{ \AA}^3$ . It is of interest to compare the crystal packing (similarities/differences) and the energetic features associated with the formation of these polymorphs.

**Crystal packing in AC-3 Form I.** The crystal structure of Form I involves the formation of molecular chains, utilizing the packing motif 1, having the highest energetic stabilization ( $-8.0 \text{ kcal mol}^{-1}$ ), linked *via* strong  $\text{N-H}\cdots\text{O}=\text{C}$  along with weak  $\text{C-H}\cdots\text{O}$  hydrogen bonds, utilizing  $c$ -glide as the symmetry element in the crystal structure [Fig. 4(c)]. The chain is then linked *via* weak  $C(sp^2)\text{-H}\cdots\text{F}$  hydrogen bonds (motif 3,  $-2.3 \text{ kcal mol}^{-1}$ ),  $\text{C-H}\cdots\pi$  (motif 4, I.E. =  $-1.6 \text{ kcal mol}^{-1}$ ) and weak  $C(sp^3)\text{-H}\cdots\text{F}$  hydrogen bonds (motif 6,  $-0.7 \text{ kcal mol}^{-1}$ ), generating a molecular sheet down the  $bc$  plane [Fig. 4(c)]. The molecules in the crystal are stacked along the crystallographic  $a$ -axis (motif 2,  $-3.7 \text{ kcal mol}^{-1}$ ) and forms a layered arrangement which is then linked *via* weak  $C(sp^3)\text{-H}\cdots\text{F}$  hydrogen bonds [motif 5,  $-0.9 \text{ kcal mol}^{-1}$ , and motif 6,  $-0.7 \text{ kcal mol}^{-1}$ , Fig. 4(d)].

**Crystal packing in AC-3 Form II.** Packing in the crystal structure displays formation of molecular chain along the crystallographic  $a$ -axis *via* strong  $\text{N-H}\cdots\text{O}=\text{C}$  along with weak  $C(sp^2)\text{-H}\cdots\text{O}=\text{C}$  (motif 1,  $-8.8 \text{ kcal mol}^{-1}$ , with mostly coulombic contribution) H-bonds. The molecular chain is connected with  $C(sp^3)\text{-H}\cdots\text{F}$  H-bonds (motif 5,  $-0.8 \text{ kcal mol}^{-1}$ ) utilizing the  $c$ -glide plane [Table 4, Fig. 4(f)]. The bifurcated  $C(sp^2)\text{-H}\cdots\text{F}$  (motif 4, I.E. =  $-2.2 \text{ kcal mol}^{-1}$  with major contribution from dispersion), is involved in the formation of "zig-zag chains" along the crystallographic  $b$ -axis

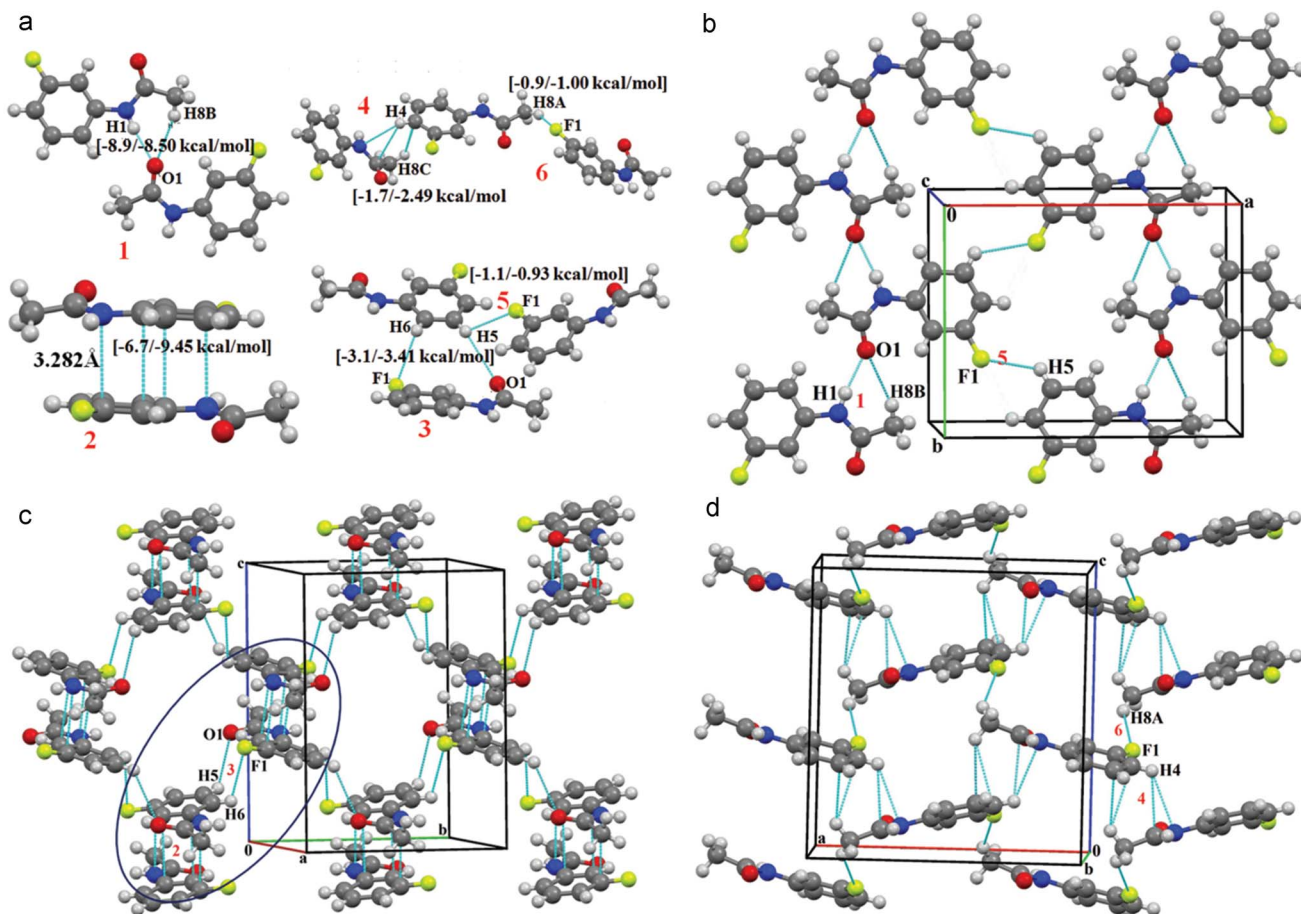


**Fig. 3** (a) Selected molecular pairs (labelled with red numbers) with their interaction energies calculated with PIXEL and DFT-D3 (Table 4) calculations in **AC-2**. (b) Packing of molecules viewed down the *ab* plane forming a molecular sheet with N-H...O=C, C-H...O=C and C-H...F hydrogen bonds in **AC-2**. (c) Packing view down the *bc* plane depicting aromatic stacking interactions in **AC-2**. (d) Packing view down the *ac* plane in **AC-2** via the network of weak C-H...N- $\pi$  and C-H...F hydrogen bonds.

(utilizing  $2_1$  screw axis as the symmetry element). The weak C(sp<sup>3</sup>)-H...O=C, along with C-H... $\pi$  (motif 3, I.E. = -5.2 kcal mol<sup>-1</sup> with the dispersion contribution being double the coulombic contribution) interconnect the “zig-zag chains” [Fig. 4(g)]. The dimeric motif 2 (I.E. = -6.6 kcal mol<sup>-1</sup>) arranges as a zig zag chain running along crystallographic *c*-axis with the utilization of bifurcated C(sp<sup>2</sup>)-H...F (motif 4, I.E. = -2.2 kcal mol<sup>-1</sup>) and C(sp<sup>3</sup>)-H...F H-bonds (motif 5, -0.8 kcal mol<sup>-1</sup>) [Fig. 4(h)].

The molecular conformation of Form II is found to be similar to the isolated molecule in the gaseous state with an approximately planar arrangement, while the phenyl ring in Form I displays a torsion twist of about 19° from the plane of the amide bond (Table 2). The lattice energy calculations indicate that Form II is 5 kcal more stable than the previously reported Form I, the difference in coulombic contribution being the most significant contributor towards the lattice energy (Table 3). The most stabilizing motif 1 (connected with strong N-H...O=C H-bonds) in both polymorphs contributes a similar amount of stabilization to the crystal structure (Table 4) but are different in terms of the orientation of the two molecules in motif 1 [Fig. 4(b) and (e)]. The extra

stabilization in Form II essentially comes from the presence of motif 3 (connected with weak C-H...O and C-H... $\pi$  H-bonds, -5.2 kcal mol<sup>-1</sup>) but these are absent in Form I. Also the motif 2 in Form II [anti-parallel stacking of molecules was observed, Fig. 4(e)] was found to be 3 kcal mol<sup>-1</sup> more stable than that in Form I [wherein parallel stacking of molecules was observed, Fig. 4(b)].

### 5. *N*-(2-(Trifluoromethyl)phenyl)acetamide (AC-4)

The molecule **AC-4** crystallizes in the centrosymmetric monoclinic space group  $P2_1/c$  with  $Z = 4$ , having intra-molecular N1-H1...F3 hydrogen bond [Fig. S5(e), ESI†]. The strong N-H...O=C along with weak C(sp<sup>3</sup>)-H...O=C, C(sp<sup>3</sup>)-F...O=C and weak C(sp<sup>3</sup>)-F...F-C(sp<sup>3</sup>) generates the most stabilized molecular pair (motif 1, I.E. = -9.1 kcal mol<sup>-1</sup>) in the crystal, which propagates along the crystallographic *a*-axis. The molecular chains thus formed are connected with weak bifurcated C(sp<sup>3</sup>)-H...F-C(sp<sup>3</sup>) hydrogen bonds [motif 6 (-1.4 kcal mol<sup>-1</sup>) and 7 (-0.9 kcal mol<sup>-1</sup>)] generating molecular sheets down the *ab* plane [Fig. 5(b)]. The packing of molecules in the third direction involves the formation of weak bifurcated weak C(sp<sup>2</sup>)-H...F-C(sp<sup>3</sup>) hydrogen bonds (motif 5, I.E. = -2.7 kcal

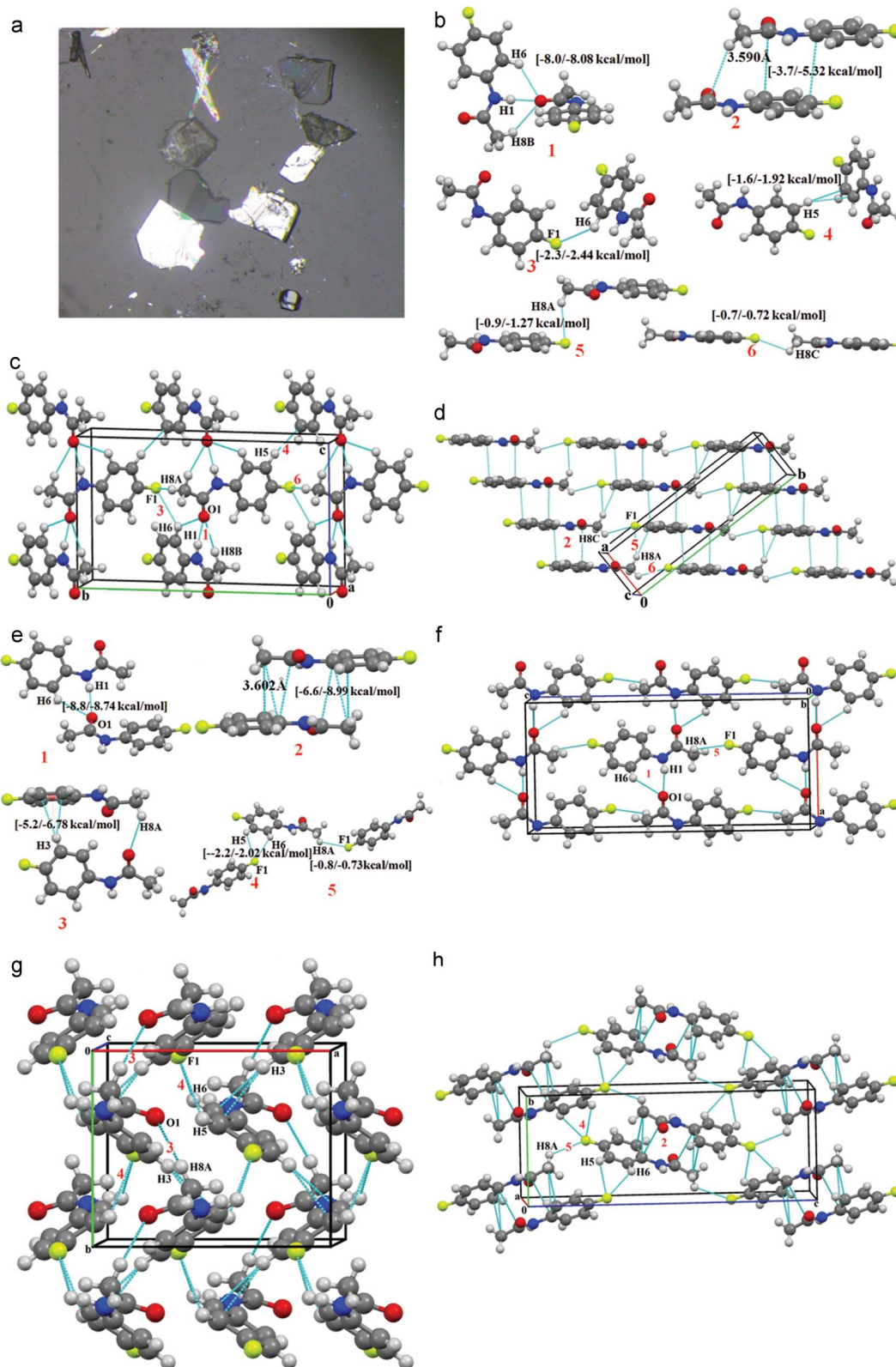


**Fig. 4** (a) Plate crystal (**Form II**) from ether solution at low temperature in **AC-3**. (b) Molecular pairs with their interaction energies from PIXEL and DFT-D3/B-97D calculations (Table 4) in **AC-3** (**Form I**). (c) Packing of molecules in **AC-3** (**Form I**) down the *bc* plane. (d) Packing view down the *ab* plane, depicting the formation of a molecular layer in **AC-3** (**Form I**). (e) Selected molecular pairs (denoted as red numbers) with interaction energies from PIXEL and DFT-D3/B-97D calculations (Table 4) in the molecular crystal of **AC-3** (**Form II**). (f) Packing view down the *ac* plane, showing N-H...O=C hydrogen bonds along with weak C(sp<sup>3</sup>)-H...F H-bonds in **AC-3** (**Form II**). (g) Packing view down the *ab* plane, depicting C-H...O=C, C-H... $\pi$  and C-H...F hydrogen bonds in **AC-3** (**Form II**). (h) Stacking interactions involving dimeric motif 2 down the *bc* plane, connected via weak C-H...F hydrogen bonds in **AC-3** (**Form II**).

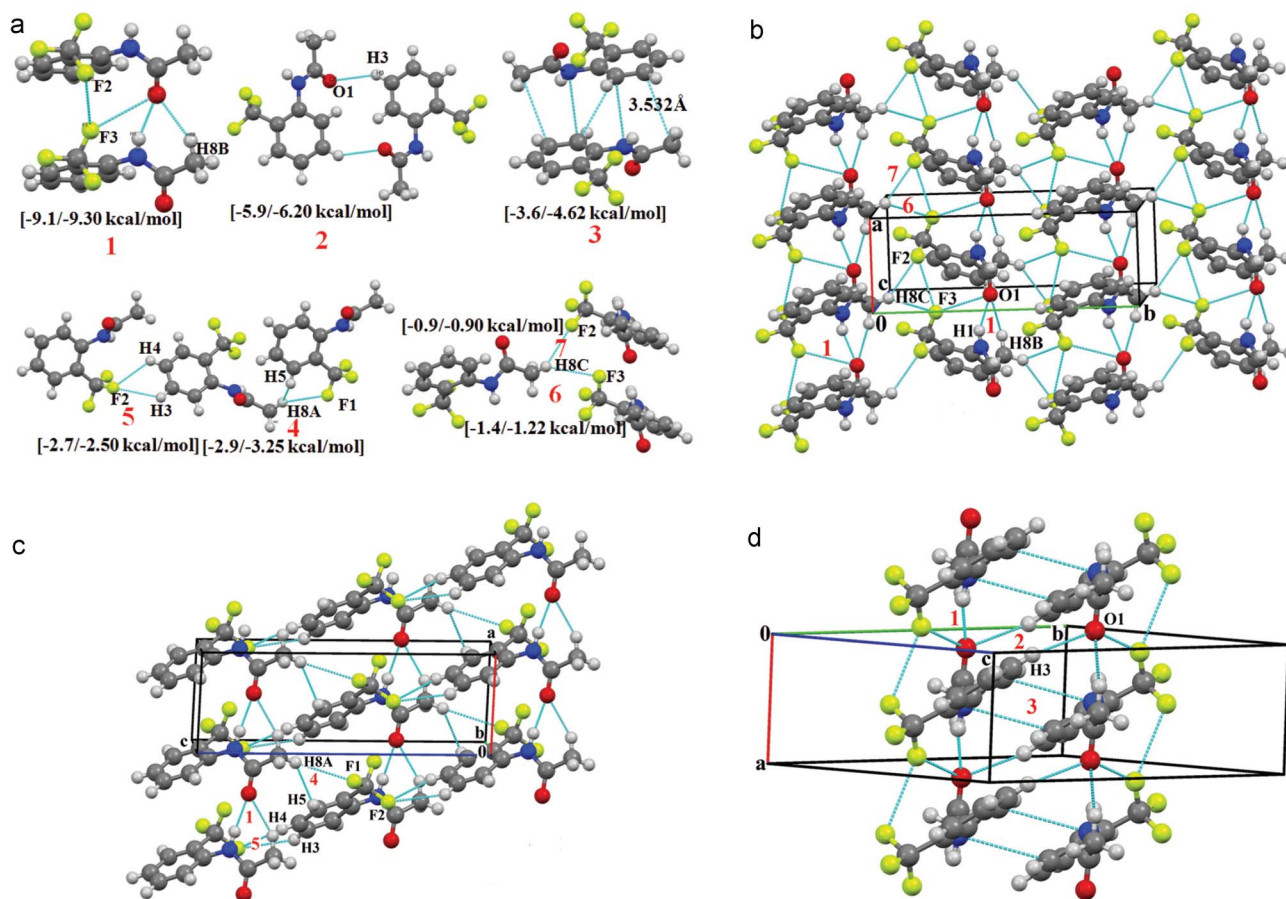


**Fig. 5** (a) Selected molecular pairs in the packing of **AC-4** along with their interaction energies from PIXEL and DFT-D3/B97-D calculations (Table 4). (b) Packing of **AC-4** down the *ab* plane, displaying network of strong N-H $\cdots$ O=C along with weak C-H $\cdots$ O, C-H $\cdots$ F hydrogen bonds and C(sp<sup>3</sup>)-F $\cdots$ F-C(sp<sup>3</sup>) contacts. (c) Packing view down the *ac* plane, depicting packing of molecules *via* strong N-H $\cdots$ O=C, weak C-H $\cdots$ O=C and C(sp<sup>2</sup>)-H $\cdots$ F-C(sp<sup>3</sup>) hydrogen bonds. (d) Packing view in **AC-4**, displaying strong N-H $\cdots$ O=C, weak C-H $\cdots$ O=C hydrogen bonds, weak C(sp<sup>3</sup>)-F $\cdots$ F-C(sp<sup>3</sup>) interactions and intermolecular stacking.

mol<sup>-1</sup> with contribution from dispersion interaction energy towards the crystal stabilization) and the occurrence of a “rare” motif 4 [Fig. 5(c)]. This motif 4 consists of one C(sp<sup>3</sup>)-H $\cdots$ F (2.86 Å, 157°, Table S2†) and C-H $\cdots$ H (relatively more acidic H5 due to presence of CF<sub>3</sub> group with C(sp<sup>3</sup>)-H8C, 2.28 Å,  $\angle$ C5-H5 $\cdots$ H8C = 129°,  $\angle$ C8-H8C $\cdots$ H5 = 142°), H $\cdots$ H contributing 2.9 kcal mol<sup>-1</sup> towards the stabilization with dispersion having a major contribution (-2.3 kcal mol<sup>-1</sup>) along with a significant contribution from coulombic and polarization (-1.8 kcal mol<sup>-1</sup>) energies. The second most stabilized molecular motifs in the crystal are the molecular pair formed *via* dimeric weak C-H $\cdots$ O=C hydrogen bonds [motif 2, I.E. = -5.9 kcal mol<sup>-1</sup> with comparable contribution from dispersion (-4.4 kcal mol<sup>-1</sup>) and coulombic energy (-3.3 kcal mol<sup>-1</sup>), Table 4]. Finally, the stacked molecular dimer (motif 3, I.E. = -3.6 kcal mol<sup>-1</sup> with mostly dispersion contribution, Table 4) also contributes towards the stability of the crystal packing [Fig. 5(d)].

## 6. N-(3-(Trifluoromethyl)phenyl)acetamide (AC-5)

The compound crystallizes in centrosymmetric monoclinic *P2<sub>1</sub>/c* space group with *Z* = 4 with an intra-molecular C2-

H2 $\cdots$ O=C hydrogen bond [Fig. S5(f), ESI†]. The strong N-H $\cdots$ O=C along with weak C-H $\cdots$ O=C hydrogen bonds (motif 1, I.E. = -8.7 kcal mol<sup>-1</sup>) participate in the formation of a molecular chain *via* 2<sub>1</sub> screw along the crystallographic *b*-axis [Fig. 6(b)]. The chains are then interconnected with the presence of motif 2 (dimeric C=O $\cdots$ C=O dipolar interactions, I.E. = -5.8 kcal mol<sup>-1</sup>), motif 3 (dimeric C=O $\cdots$ O=C along with C8-H8A $\cdots$ O=C hydrogen bond, I.E. = -5.6 kcal mol<sup>-1</sup>) and motif 4 ( $\pi\cdots\pi$  interaction, I.E. = -5.3 kcal mol<sup>-1</sup>) [Fig. 6(b)]. It is to be noted that the molecular pairs consisting of C=O dimeric motifs are the second and third most stabilizing motif in the crystal with significant coulombic contributions<sup>40</sup> (Table 4). The packing in the crystal also displays the formation of molecular layers down the *ac* plane with the -CF<sub>3</sub> moieties approaching each other. These result in the formation of motifs 5, 6, 7, 8 [Fig. 6(b) and 6(c)]. The analysis of these brings out some interesting results. Although the motif 5 consists of dimeric C(sp<sup>2</sup>)-H $\cdots$ F-C(sp<sup>3</sup>) (2.76 Å, 136°) along with a C(sp<sup>3</sup>)-F $\cdots$ F-C(sp<sup>3</sup>) (2.988 Å) interaction (present diagonally in dimeric motif) contribute 1.5 kcal mol<sup>-1</sup> to the stabilization, the same kind of C(sp<sup>2</sup>)-H $\cdots$ F-C(sp<sup>3</sup>) in motif 6 (2.83 Å, 124°) also contributes 1.5 kcal to the stabilization

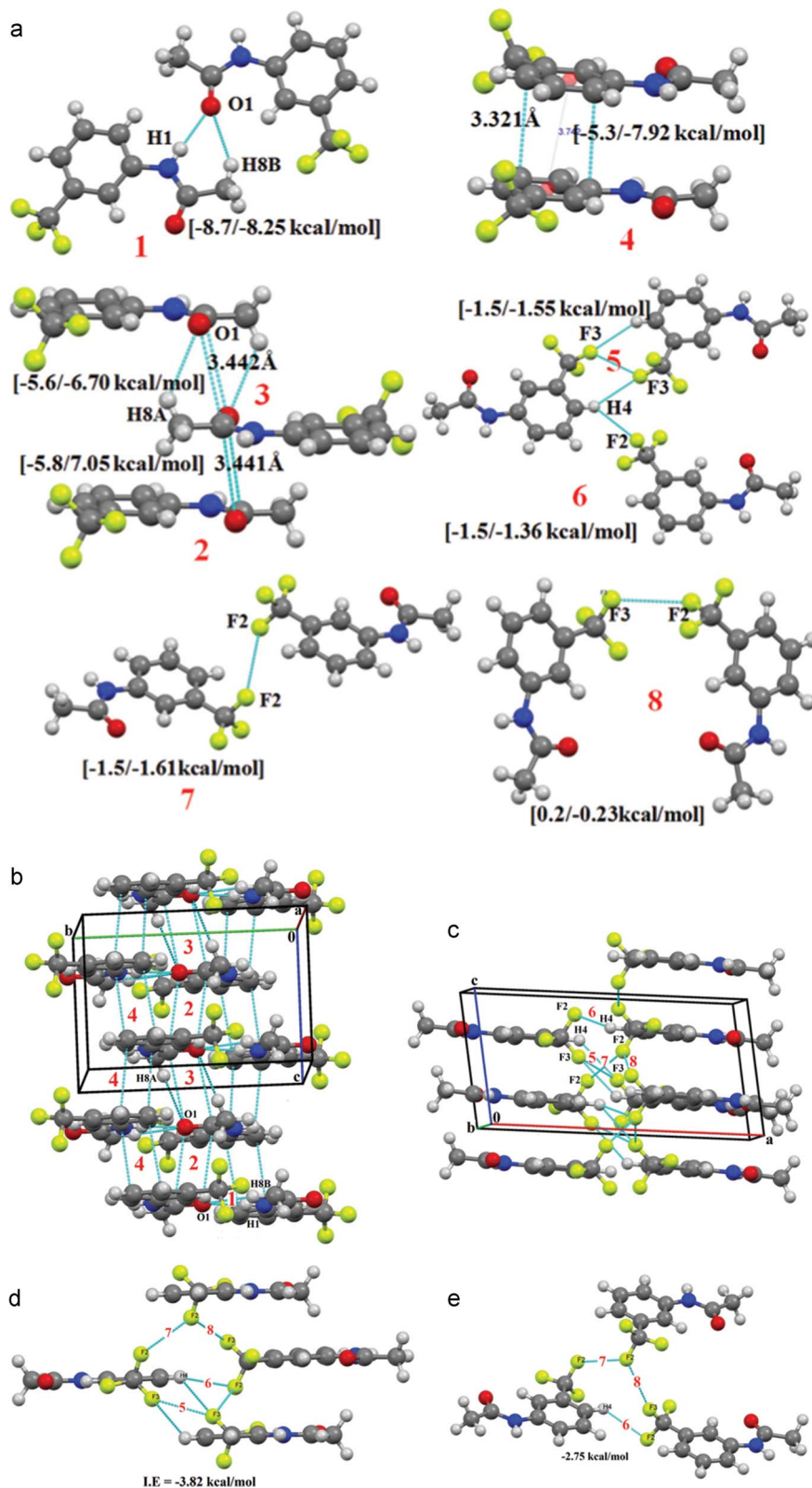


**Fig. 6** (a) Molecular pairs present in the crystal packing with their interaction energies from PIXEL and DFT-D3/B97-D calculations (Table 4) in **AC-5**. (b) Packing of molecules down the *bc* plane in **AC-5** via N-H...O=C, weak C-H...O=C hydrogen bonds and stacking interactions. (c) Packing view down the *ac* plane via weak C(sp<sup>2</sup>)-H...F-C(sp<sup>3</sup>) hydrogen bonds and C(sp<sup>3</sup>)-F...F-C(sp<sup>3</sup>) contacts in **AC-5**. (d) Formation of tetrameric motif in **AC-5**. (e) Formation of trimeric motif in **AC-5** connected via C-H...F and F...F contacts.

(Table 4). The calculations from the isolated pair for motif 6 suggest that it is less stable by  $0.2 \text{ kcal mol}^{-1}$  than motif 5. This confirms that the extra stabilization of motif 6 comes from crystal packing. It is to be noted that the interaction energy of motif 7 consisting of  $\text{C}(\text{sp}^3)\text{-F}2\cdots\text{F}2\text{-C}(\text{sp}^3)$  ( $3.096 \text{ \AA}$ ,  $\theta_1 = \theta_2 = 122^\circ$ ) is found to be  $-1.5 \text{ kcal mol}^{-1}$  (isolated pair I.E. =  $-1.61 \text{ kcal mol}^{-1}$ ) with dispersion as a major contributor towards stabilization. It is to be noted that motif 8, although geometrically similar [ $\text{C}(\text{sp}^3)\text{-F}\cdots\text{F-C}(\text{sp}^3)$  =  $3.113 \text{ \AA}$ ,  $\theta_1 = 118^\circ, \theta_2 = 113^\circ$ ] to motif 7, does contribute towards the crystal packing. The energy is positive, hence depicting the slightly repulsive nature associated with  $\text{F}\cdots\text{F}$  interaction. This may be attributed to the repulsion, owing to the arrangement and orientation of the C-F bond dipole moments with respect to each other in the crystal environment. In order to evaluate the additive nature of these interaction energies, we performed DFT-D3/B97-D calculations to obtain the total interaction energy for the tetrameric motif [I.E. =  $E_{\text{tetramer}} - 4 \times E_{\text{monomer}}$ , Fig. 6(d), consisting of the molecular motifs 5, 6, 7 and 8]. This confers an overall stabilization of  $-3.81 \text{ kcal mol}^{-1}$ . Similar calculations performed on the molecular trimer, having motifs 6, 7 and 8, provide stabilization to the extent of  $-2.75 \text{ kcal mol}^{-1}$ .

### 7. *N*-(4-(Trifluoromethyl)phenyl)acetamide (AC-6)

The compound AC-6 crystallizes in centrosymmetric orthorhombic space group *Pbca* with  $Z = 8$  [Fig. S5(g), ESI†]. As is observed in the previous cases, the stabilizing molecular pair consist of strong  $\text{N-H}\cdots\text{O}=\text{C}$  along with weak  $\text{C-H}\cdots\text{O}=\text{C}$  hydrogen bonds (motif 1, I.E. =  $-8.1 \text{ kcal mol}^{-1}$ ). These are involved in the formation of molecular chains along the *a*-glide perpendicular to the crystallographic *c*-axis. The chains are interconnected with weak  $\text{C}(\text{sp}^2)\text{-H}\cdots\text{F-C}(\text{sp}^3)$  hydrogen bonds along with  $\text{C}(\text{sp}^3)\text{-F}\cdots\text{F-C}(\text{sp}^3)$  interactions (motif 3 and 5) [Fig. 7(b)]. The molecules in the crystal stack together resulting in the formation of a molecular ladder [Fig. 7(c)]. The weak  $\text{C}(\text{sp}^3)\text{-H}\cdots\text{F-C}(\text{sp}^3)$  (motif 4) connect the molecular ladder in a zig zag manner along the *c*-axis.

The motif 2 (stacking of molecules) contributes  $5.5 \text{ kcal mol}^{-1}$  towards the stabilization of the crystal packing ( $1.5 \text{ kcal mol}^{-1}$  less stable compared to DFT calculations, the I.E. is  $-7.02 \text{ kcal mol}^{-1}$ ). Motif 3 and motif 5 are found to be similar to motif 5 in AC-5, these contributing  $1.8 \text{ kcal mol}^{-1}$  and  $1.0 \text{ kcal mol}^{-1}$  towards the stabilization, with the major contribution coming from the dispersion energy, attributed primarily to  $\text{C-H}\cdots\text{F}$  H-bonds in these motifs (Table 4). It is actually the increased repulsion contribution in this case of AC-6 (wherein the interatomic distances involving fluorine atoms are less than the sum of van der Waals radii, Tables S2 and S3, ESI†), compared to that in AC-5, wherein the distance between the interacting fluorine atoms in motif 5 is greater than the sum of van der Waals radii that results in decreased repulsion, although these represent similar type of motifs (Table 4). Motif 4, formed with short and directional  $\text{C}(\text{sp}^3)\text{-H}\cdots\text{F-C}(\text{sp}^3)$  ( $2.66 \text{ \AA}$ ,  $165^\circ$ ), contributes  $-1.4 \text{ kcal mol}^{-1}$  towards the stabilization of crystal structure.

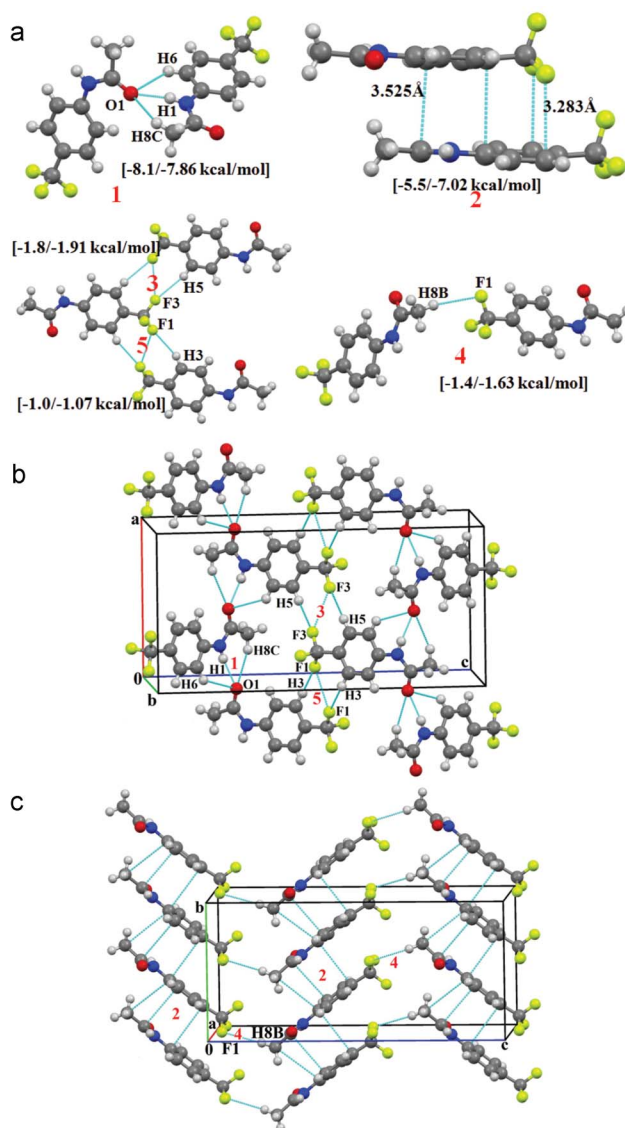


**Fig. 7** (a) Molecular pairs along with their interaction energies from PIXEL and DFT-D3/B97-D calculations (Table 4) in AC-6. (b) Packing view down the *ac* plane, displaying  $\text{N-H}\cdots\text{O}=\text{C}$ , weak  $\text{C}(\text{sp}^2)\text{-H}\cdots\text{O}=\text{C}$ ,  $\text{C}(\text{sp}^2)\text{-H}\cdots\text{F-C}(\text{sp}^3)$  hydrogen bonds along with  $\text{C}(\text{sp}^3)\text{-F}\cdots\text{F-C}(\text{sp}^3)$  interactions in AC-6. (c) Formation of molecular ladder down the *bc* plane in AC-6 via stacking interactions and  $\text{C}(\text{sp}^3)\text{-H}\cdots\text{F-C}(\text{sp}^3)$  hydrogen bonds.

### 8. *N*-Methylbenzamide (BZ-0)

The compound crystallizes in centrosymmetric orthorhombic space group *Pbca* with  $Z = 8$  [Fig. S5(h), ESI†]. The most stabilized motif 1, formed with strong  $\text{N-H}\cdots\text{O}=\text{C}$  along with weak  $\text{C}(\text{sp}^2)\text{-H}\cdots\text{O}=\text{C}$  hydrogen bonds, provides  $-8.8 \text{ kcal mol}^{-1}$ . This motif forms molecular chains along the crystallographic *a*-axis utilizing the  $2_1$  screw axis as the symmetry element. The parallel chains are interconnected [Fig. 8(b)] utilizing the stacking interactions (motif 2, I.E. =  $-6.0 \text{ kcal mol}^{-1}$ ) forming molecular sheets which are further stabilized via weak  $\text{C}(\text{sp}^3)\text{-H}\cdots\text{O}=\text{C}$  hydrogen bonds (motif 3, I.E. =  $-4.2 \text{ kcal mol}^{-1}$  with dispersion energy as a major contributor) propagating along the *b* axis in the crystal structure. The motif

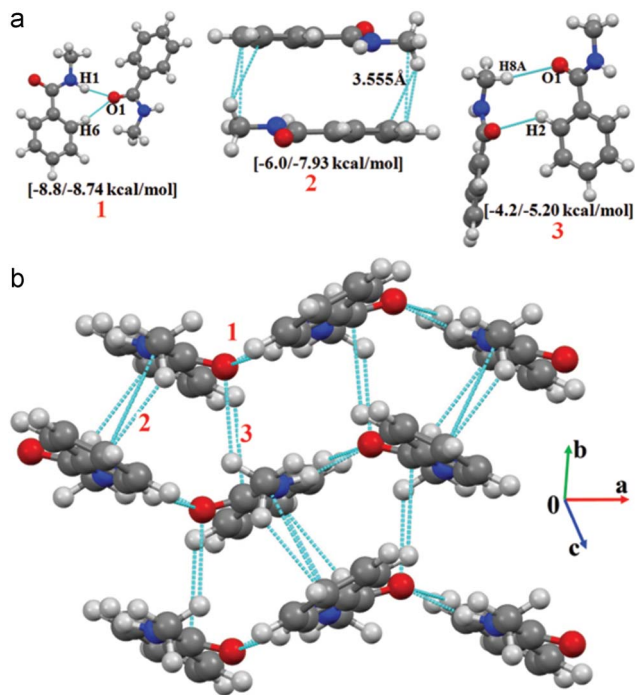


**Fig. 8** (a) Molecular pairs with their interaction energy from PIXEL and DFT-D3/B97-D calculations (Table 4) in **BZ-0**. (b) Packing of molecule in crystal *via* N-H $\cdots$ O=C, C(sp<sup>3</sup>)-H $\cdots$ O=C, C(sp<sup>2</sup>)-H $\cdots$  $\pi$  hydrogen bonds in **BZ-0**.

2 in the crystal is 1.9 kcal mol<sup>-1</sup> is less stable than the value obtained from DFT calculations.

### 9. 2-Fluoro-*N*-methylbenzamide (BZ-1)

The molecule crystallizes in a centrosymmetric triclinic space group  $P\bar{1}$  with two molecules in the asymmetric unit [molecule A (carbon atom = grey color) and B (carbon atom = violet color)], thus having  $Z = 4$  [Fig. S5(i), ESI<sup>†</sup>] molecules in unit cell. The fluorine atom on phenyl ring in both the molecules in the asymmetric unit were found to be disordered at two positions with the occupancy ratio of 0.920(2) : 0.080(2) for molecule A and 0.921(2) : 0.079(2) for molecule B. The two molecules in the asymmetric unit are connected with strong N-H $\cdots$ O=C, weak C(sp<sup>3</sup>)-H $\cdots$ O=C and C(sp<sup>3</sup>)-H $\cdots$ F-C(sp<sup>2</sup>) hydrogen bonds (motif 3, I.E. = -6.6 kcal mol<sup>-1</sup>) and the structure is also stabilized by intra molecular N-H $\cdots$ F hydrogen bonds in both the molecules of the asymmetric unit. The asymmetric unit is connected along the crystallographic  $b$  axis with strong N-H $\cdots$ O=C, weak C(sp<sup>3</sup>)-H $\cdots$ O=C and C(sp<sup>3</sup>)-H $\cdots$ F-C(sp<sup>2</sup>) hydrogen bonds (motif 4, I.E. = -6.2 kcal mol<sup>-1</sup>) and forms molecular chains with an  $\cdots$ ABAB $\cdots$  arrangement [Fig. 9(b)]. Two such chains are interconnected with weak C(sp<sup>3</sup>)-H $\cdots$ F-C(sp<sup>2</sup>) and C(sp<sup>2</sup>)-H $\cdots$ F-C(sp<sup>2</sup>) hydrogen bonds [Fig. 9(b)], which is characterized as motif 7 in the crystal packing [Fig. 9(a)]. These contribute 2.8 kcal mol<sup>-1</sup> (Table 4), towards the stabilization of the lattice, with the major contribution coming from the dispersive component. Furthermore, both molecules of the asymmetric unit are stacked along crystallographic  $a$ -axis [motif 1 (I.E. = -5.2 kcal mol<sup>-1</sup>), 2 (I.E. = -3.9 kcal mol<sup>-1</sup>), 9 (I.E. = -4.7 kcal mol<sup>-1</sup>)

and 10 (I.E. = -3.9 kcal mol<sup>-1</sup>)] in the formation of molecular layers [Fig. 9(c)] which are connected with bifurcated C(sp<sup>2</sup>)-H $\cdots$ F-C(sp<sup>2</sup>) and C(sp<sup>3</sup>)-H $\cdots$ F-C(sp<sup>2</sup>) hydrogen bonds (motif 8, I.E. = -2.6 kcal mol<sup>-1</sup>) and weak C-H $\cdots$ O=C hydrogen bond (motif 6, I.E. = -3.0 kcal mol<sup>-1</sup>).

### 10. 3-Fluoro-*N*-methylbenzamide (BZ-2)

The compound crystallizes in the centrosymmetric orthorhombic space group  $Pbca$  with  $Z = 8$  [Fig. S5(j), ESI<sup>†</sup>]. A well defined strong N-H $\cdots$ O=C along with C(sp<sup>2</sup>)-H $\cdots$ O=C (motif 1, I.E. = -9.0 kcal mol<sup>-1</sup> with coulombic as a main contributor) directs the formation of a helical molecular chain along the 2<sub>1</sub> screw parallel to crystallographic  $a$ -axis [Fig. 10(b)]. These chains are then inter-connected with weak bifurcated C(sp<sup>2</sup>)-H $\cdots$ F hydrogen bonds (motif 5, offered 2 kcal mol<sup>-1</sup> to the stabilization with dispersion as a major contributor) propagating along the  $a$ -glide plane [Fig. 10(b)]. The weak C(sp<sup>3</sup>)-H $\cdots$ O=C hydrogen bond along with C-F $\cdots$  $\pi$  interaction (motif 3, I.E. = -3.7 kcal mol<sup>-1</sup> with major contribution from dispersion) pack utilizing the  $b$ -glide plane and are then linked *via* weak C(sp<sup>3</sup>)-H $\cdots$ F-C(sp<sup>2</sup>) (motif 6, I.E. = -1.2 kcal mol<sup>-1</sup>) H-bonds forming a ladder-like arrangement in the crystal structure [Fig. 10(c)]. The stacked dimers (motif 2, I.E. = -6.1 kcal mol<sup>-1</sup>) pack in a herringbone arrangement down the  $bc$  plane, linked with weak C(sp<sup>2</sup>)-H $\cdots$ F-C(sp<sup>2</sup>) and C-H $\cdots$  $\pi$  hydrogen bonds (motif 4, I.E. = -2.7 kcal with dispersion as major contributor).

### 11. 4-Fluoro-*N*-methylbenzamide (BZ-3)

The compound crystallizes in the centrosymmetric monoclinic space group  $Pbca$  with  $Z = 8$  [Fig. S5(k), ESI<sup>†</sup>]. The packing in the crystal structure involves the formation of molecular chains *via* strong N-H $\cdots$ O=C along with C(sp<sup>2</sup>)-H $\cdots$ O=C hydrogen bonds (motif 1, I.E. = 8.7 kcal mol<sup>-1</sup> with major coulombic contribution) along the  $b$ -glide plane. The chains are inter-linked with the presence of weak C-H $\cdots$ F hydrogen bonds (fluorine is a trifurcated acceptor) [motif 6 (I.E. = -1.6 kcal mol<sup>-1</sup>) and 7 (I.E. = -1.0 kcal mol<sup>-1</sup> with major contribution coming from dispersion)] [Fig. 11(b)]. The motif 2 (total I.E. = -4.7 kcal mol<sup>-1</sup>) are arranged as zig zag chains along the crystallographic  $c$ -axis with the utilization of C(sp<sup>2</sup>)-H $\cdots$ F-C(sp<sup>2</sup>) and C(sp<sup>3</sup>)-H $\cdots$  $\pi$  hydrogen bonds (motif 3, I.E. = -2.7 kcal mol<sup>-1</sup> with major dispersion as contribution) [Fig. 11(c)]. Additional weak C(sp<sup>3</sup>)-H $\cdots$ F-C(sp<sup>2</sup>) (motif 7, I.E. = -1.0 kcal mol<sup>-1</sup>) hydrogen bonds provide additional stability forming molecular chains along the  $a$ -axis. The packing in the crystal is also characterized by the presence of two motifs 5 and 6, comprising of weak C(sp<sup>2</sup>)-H $\cdots$ O hydrogen bonds, the stabilization provided being -2.1 and -2.0 kcal mol<sup>-1</sup> (with major contribution coming from dispersion) to the crystal packing. These form molecular chains with the utilization of a 2<sub>1</sub> screw along crystallographic  $a$ -axis and  $b$ -axis [Fig. 11(d)].

### 12. *N*-Methyl-2-(trifluoromethyl)benzamide (BZ-4)

The compound crystallizes in the centrosymmetric space group  $P2_1/c$  with  $Z = 4$  [Fig. S5(l), ESI<sup>†</sup>]. The motif 1 is characterized by the presence of strong N-H $\cdots$ O=C, weak C(sp<sup>3</sup>)-H $\cdots$ O and weak C(sp<sup>3</sup>)-H $\cdots$  $\pi$  hydrogen bonds along

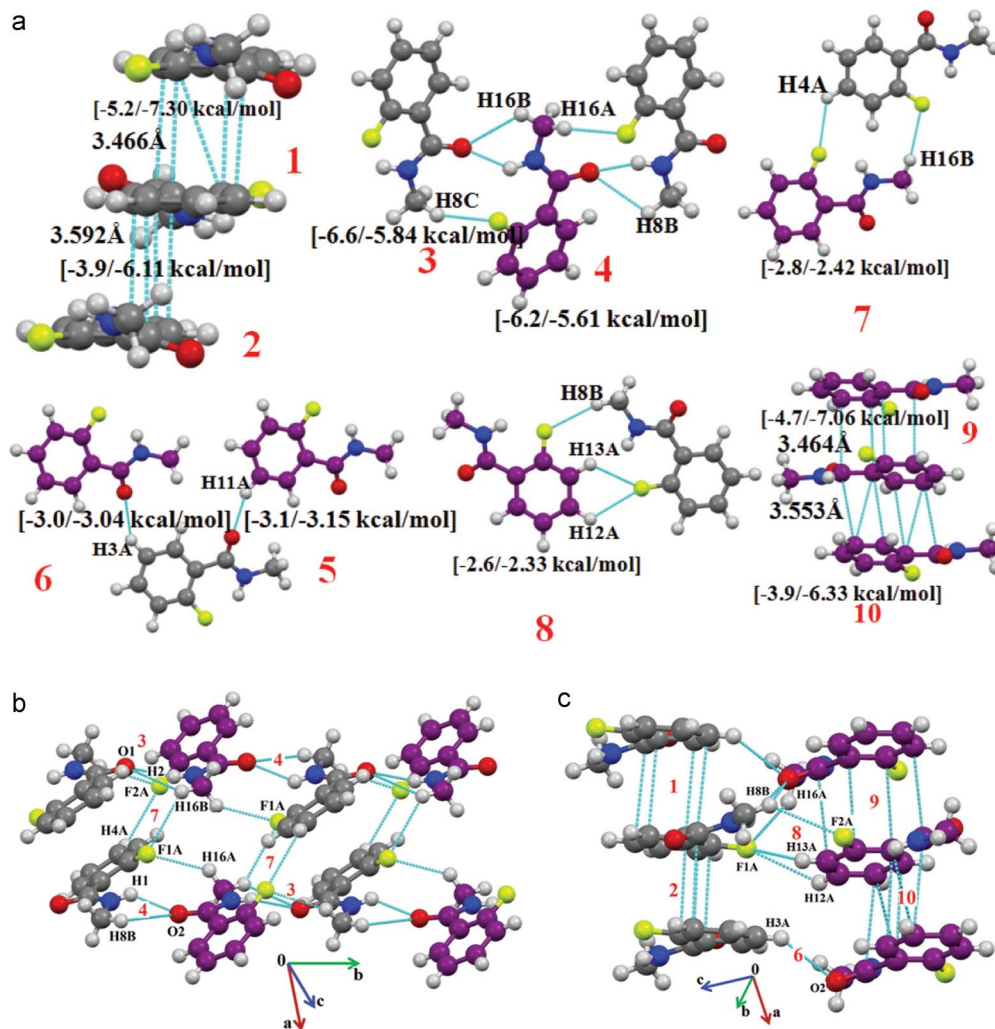


**Fig. 9** (a) Molecular pairs with their interaction energies calculated from PIXEL and DFT-D3 (Table 4) in **BZ-1**. (b) Packing view depicting strong N-H...O, weak C-H...O, C-H...F hydrogen bonds in **BZ-1**. (c) Packing view depicting formation molecular layer *via* stacking, weak C-H...O, C-H...F hydrogen bonds in **BZ-1**.

with  $C(sp^3)-F\cdots F-C(sp^3)$  interaction, [Fig. 12(b)] contribute  $-8.3 \text{ kcal mol}^{-1}$  towards the crystal stabilization, propagating along the *c*-glide plane. The molecular chains thus formed are inter linked with  $C(sp^2)-H\cdots O$ , weak  $C(sp)-H\cdots\pi$  (motif 3, I.E. =  $-3.8 \text{ kcal mol}^{-1}$  with dispersion as a major contributor) also propagating along the *c*-glide plane [Fig. 12(b)]. It is to be noted that the second greatest contributor to the stabilization of the crystal structure is the molecular pair connected with short and directional ( $2.37 \text{ \AA}$ ,  $153^\circ$ ) (Table S2†)  $C(sp^2)-H\cdots O$  dimeric hydrogen bonds (motif 2, I.E. =  $-7.0 \text{ kcal mol}^{-1}$ , with major coulombic contribution as  $-5.3 \text{ kcal mol}^{-1}$ ). The weak  $C(sp^2)-H\cdots F-C(sp^3)$  along with  $C(sp^3)-F\cdots F-C(sp^3)$  (motif 5, I.E. =  $2.6 \text{ kcal mol}^{-1}$  with major dispersion contribution, Table 4) generates a molecular chain utilizing the  $2_1$  screw along the crystallographic *b*-axis [Fig. 12(c)]. Such chains are then interconnected *via* the dimeric motif 2. The packing in the crystal also consists of the presence of another dimeric molecular pair connected with short and directional ( $2.59 \text{ \AA}$ ,  $147^\circ$ ) (Table S2†) weak  $C(sp^2)-H\cdots F-C(sp^3)$  hydrogen bonds [Fig. 12(d)] (motif 4), which contribute  $2.7 \text{ kcal mol}^{-1}$  to the

stabilization of crystal with the major contribution coming from dispersion (Table 4).

### 13. *N*-Methyl-3-(trifluoromethyl)benzamide (**BZ-5**)

The molecule crystallizes in the centrosymmetric monoclinic space group  $P2_1/c$  with  $Z = 4$  [Fig. S5(m), ESI†]. The packing in the crystal structure involves the formation of a molecular ribbon by strong  $N-H\cdots O=C$  and weak  $C-H\cdots O=C$  hydrogen bonds along the  $2_1$  screw parallel to the crystallographic *b*-axis (motif 1, I.E. =  $-8.7 \text{ kcal mol}^{-1}$ ) [Fig. 13(b)]. The packing of molecules in the crystal is also characterized by the presence of dipole-dipole interactions of the carbonyl group ( $>C=O$ ) of the molecule which contribute  $5.6 \text{ kcal mol}^{-1}$  (major contribution coming from dispersion) to the stabilization of the crystal (motif 3, Table 4). Such a molecular pair (motif 3) arranges as molecular layers parallel to the *ac* plane *via* weak  $C(sp^3)-H\cdots O$  hydrogen bonds forming dimers (motif 4, I.E. =  $-4.6 \text{ kcal mol}^{-1}$ ) [Fig. 13(c)]. The layers thus formed are then connected with weak  $C(sp^3)-F\cdots F-C(sp^3)$  interactions (motifs 5 and 7) [Fig. 13(c)] forming the characteristic ribbon-like motif.

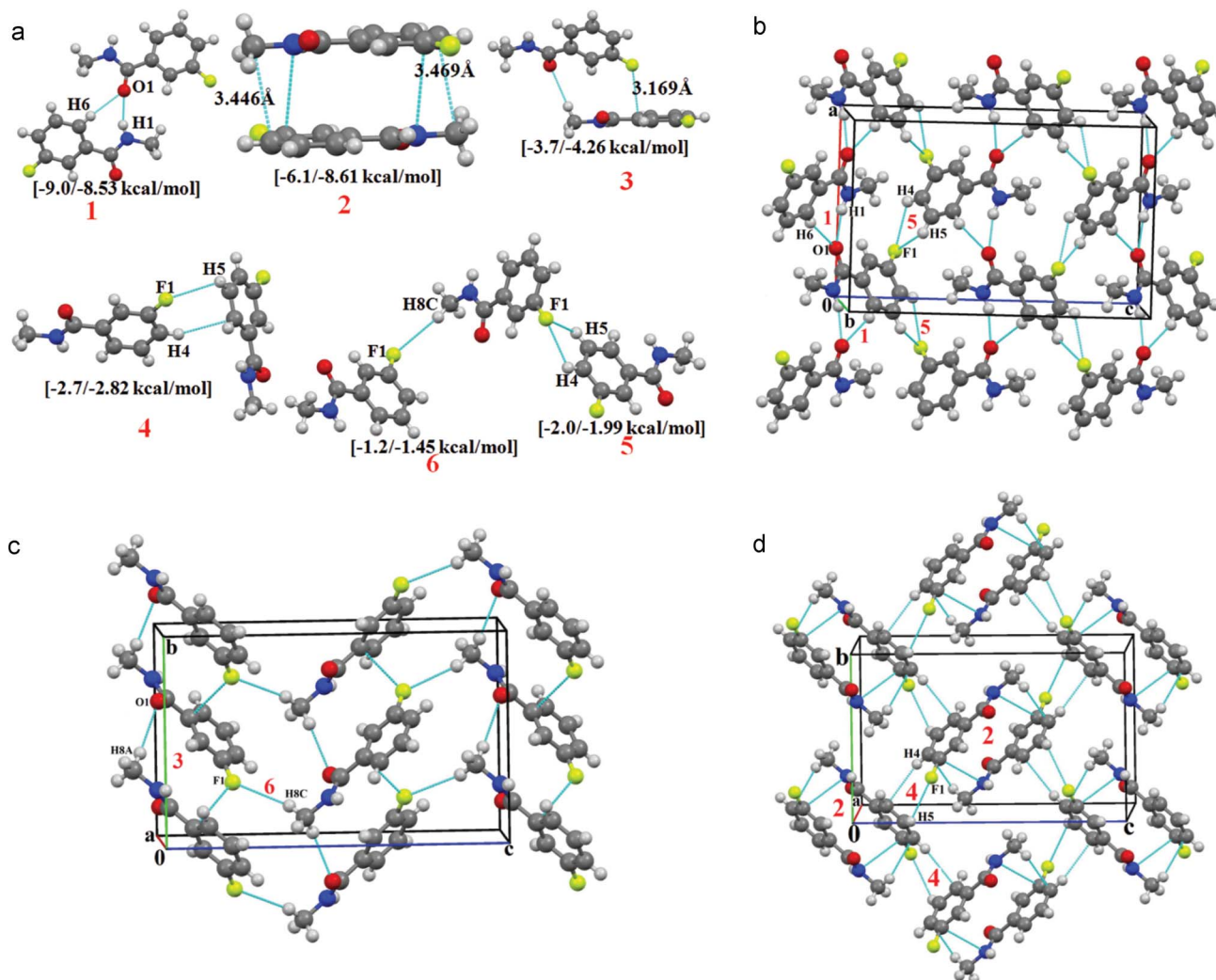


**Fig. 10** (a) Selected molecular pairs in the crystal structure of **BZ-2** with their interaction energy obtained with PIXEL and DFT-D3 calculation (Table 4). (b) Packing view down the *ac* plane displaying network of  $\text{N-H}\cdots\text{O}=\text{C}$ ,  $\text{C}(\text{sp}^2)\text{-H}\cdots\text{O}=\text{C}$ ,  $\text{C}(\text{sp}^2)\text{-H}\cdots\text{F}$  hydrogen bonds in **BZ-2**. (c) Packing view down the *bc* plane showing weak  $\text{C}(\text{sp}^3)\text{-H}\cdots\text{O}=\text{C}$ ,  $\text{C}(\text{sp}^3)\text{-H}\cdots\text{F}-\text{C}(\text{sp}^2)$  hydrogen bonds along with  $\text{C-F}\cdots\pi$  interaction in the crystal packing of **BZ-2**. (d) Packing view down the *bc* plane, showing formation of the herringbone arrangement in the crystal packing of **BZ-2**.

The packing of the molecules are also characterized by the presence of stacking interactions along the *c*-glide plane which contribute  $5.6 \text{ kcal mol}^{-1}$  (motif 2) to the stabilization [Fig. 13(d)]. It is to be noted that motif 5 consists of dimeric  $\text{C9}(\text{sp}^3)\text{-F2}\cdots\text{F3}-\text{C9}(\text{sp}^3)$  ( $3.072 \text{ \AA}$ ,  $\theta_1 = 90^\circ$ ,  $\theta_2 = 127^\circ$ ) and  $\text{C9}(\text{sp}^3)\text{-F3}\cdots\text{F3}-\text{C9}(\text{sp}^3)$  ( $3.007$ ,  $\theta_1 = \theta_2 = 93^\circ$ ) interactions. These contribute  $2 \text{ kcal mol}^{-1}$  (Table S3, ESI† and Table 4) towards the stabilization of the crystal, which is slightly higher than the stabilization coming from motif 6, consisting of two  $\text{C-H}(\text{sp}^2)\cdots\text{F}-\text{C}(\text{sp}^3)$  hydrogen bonds. The dimeric  $\text{C9}(\text{sp}^3)\text{-F1}\cdots\text{F3}-\text{C9}(\text{sp}^3)$  ( $3.018 \text{ \AA}$ ,  $\theta_1 = 132^\circ$ ,  $\theta_2 = 112^\circ$ ) (Table S3†) are also found to be stabilized by  $-1.1 \text{ kcal mol}^{-1}$ . The calculation for the isolated pairs also gave similar results for these fluorine interactions<sup>41</sup> (Table 4). The DFT-D3/B97-D calculation of total interaction energy of tetrameric motif [Fig. 13(e)] gave an overall stabilization by  $-3.39 \text{ kcal mol}^{-1}$ .

#### 14. *N*-Methyl-3-(trifluoromethyl)benzamide (**BZ-6**)

The compound **BZ-6** crystallizes in the centrosymmetric monoclinic space group  $P2_1/n$  [Fig. S5(n), ESI†]. The packing in the crystal structure involves formation of molecular sheets with the utilization of a strong  $\text{N-H}\cdots\text{O}=\text{C}$  (motif 1,  $-9.6 \text{ kcal mol}^{-1}$ ) down the *ab* plane [Fig. 14(b)]. It is of interest to note the occurrence of motif 7 in the crystal packing (the  $\text{CH}_3$  and  $\text{CF}_3$  group come close to each other, thus these provide  $1.4 \text{ kcal mol}^{-1}$  of stabilization, with the dispersion being the major contribution), which forms the molecular chain along the *b*-axis in the crystal structure [Fig. 14(b)]. The packing also displays the formation of a molecular sheet with the utilization of weak  $\text{C-H}\cdots\text{O}$  along with  $\text{C}(\text{sp}^2)\text{-H}\cdots\text{F}-\text{C}(\text{sp}^3)$  (motif 3, I.E. =  $-3.3 \text{ kcal mol}^{-1}$ ) utilizing a  $2_1$  screw along the *b*-axis and weak dimeric  $\text{C}(\text{sp}^2)\text{-H}\cdots\text{F}-\text{C}(\text{sp}^3)$  hydrogen bonds (motif 6, provides  $2.3 \text{ kcal mol}^{-1}$  to the stabilization) [Fig. 14(c)]. The second most stabilizing dimeric motif 2 [Fig. 14(a), molecular pair

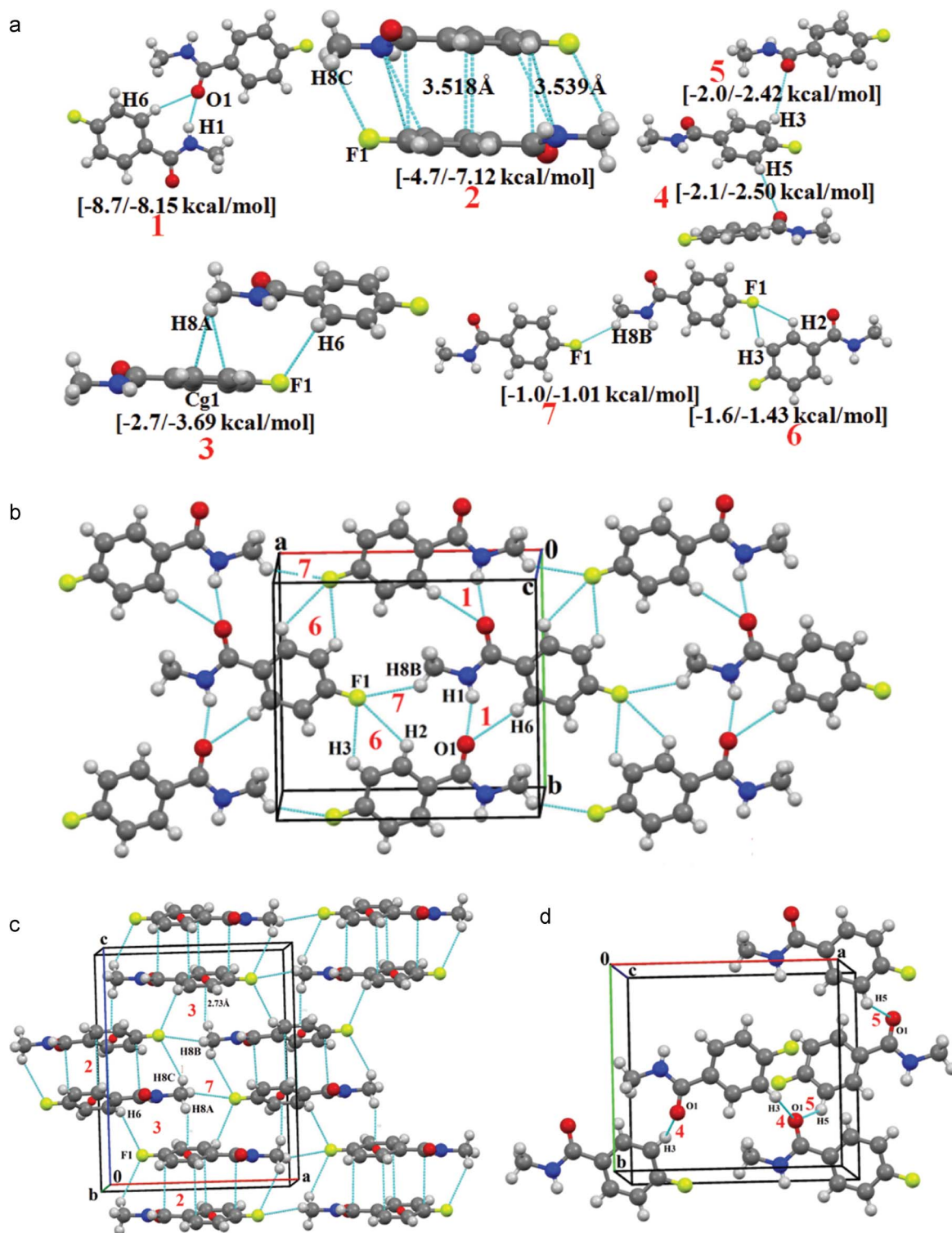


**Fig. 11** (a) Depiction of molecular pairs with their interaction energies in **BZ-3** calculated from PIXEL and DFT-D3 calculation (Table 4). (b) Packing view down the *ab* plane displaying N-H $\cdots$ O=C, C(sp<sup>2</sup>)-H $\cdots$ O=C, bifurcated C(sp<sup>2</sup>)-H $\cdots$ F and C(sp<sup>3</sup>)-H $\cdots$ F hydrogen bonds in **BZ-3**. (c) Packing view down the *ac* plane, displaying the stacking motif, C(sp<sup>2</sup>)-H $\cdots$ F, C(sp<sup>3</sup>)-H $\cdots$ F and C-H $\cdots$  $\pi$  hydrogen bonds in **BZ-3** (small red ball represents the center of gravity of phenyl ring, the big red ball represents oxygen atom). (d) Packing view down the *ab* plane depicting weak C-H $\cdots$ O hydrogen bonds in **BZ-3**.

linked *via* weak C-H $\cdots$ O and C-H $\cdots$  $\pi$  hydrogen bonds, I.E. = -7.7 kcal mol<sup>-1</sup>] arranged down the *bc* plane with motif 4 (contributing 2.8 kcal mol<sup>-1</sup> stabilization) and weak interac-

tions between the CH<sub>3</sub> $\cdots$ CF<sub>3</sub> group forming C(sp<sup>3</sup>)-H $\cdots$ F-C(sp<sup>3</sup>) H-bonds (motif 7, I.E. = -1.4 kcal mol<sup>-1</sup>) [Fig. 14(d)].

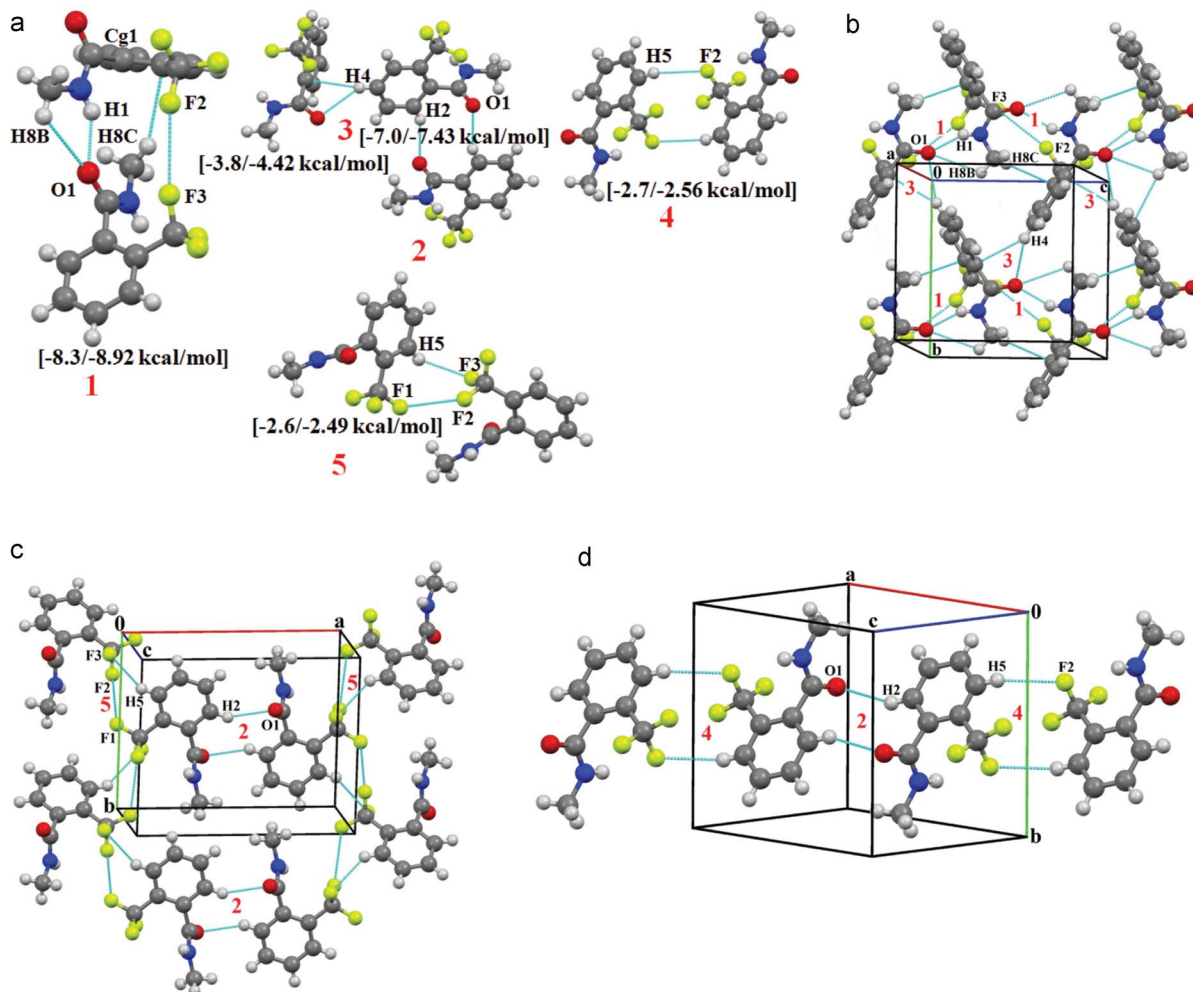


**Fig. 12** (a) Molecular pairs in the crystal structure with their total interaction energy calculated from PIXEL and DFT-D3 (Table 4) in **BZ-4**. (b) Packing view down the *bc* plane displaying N-H $\cdots$ O=C, C(sp<sup>2</sup>)-H $\cdots$ O=C, C(sp<sup>3</sup>)-H $\cdots$ O=C, C(sp<sup>3</sup>)-H $\cdots$  $\pi$  and C(sp<sup>3</sup>)-F $\cdots$ F-C(sp<sup>3</sup>) hydrogen bonds in **BZ-4**. (c) Packing view down the *ab* plane showing C-H $\cdots$ O=C, C(sp<sup>2</sup>)-H $\cdots$ F-C(sp<sup>3</sup>) hydrogen bonds and C(sp<sup>3</sup>)-F $\cdots$ F-C(sp<sup>3</sup>) intermolecular contacts in **BZ-4**. (d) Packing of molecule in **BZ-4** with C-H $\cdots$ O=C and C(sp<sup>2</sup>)-H $\cdots$ F hydrogen bonds.

A comparative study of the key supramolecular motifs, with inputs from energy calculations in these compounds reveal the following relevant discussions:

1. The energy associated with the motif 1 (containing a strong N-H $\cdots$ O=C hydrogen bond) in the crystal structures were found to be similar (the value lies within the range of  $-8$  to  $-9$  kcal mol<sup>-1</sup>, with a major contribution towards the stabilization being coulombic in origin) in the case of all the compounds. Hence the motif 1 can be considered as the main building block observed in the crystal structure of all the compounds.

2. The interaction energy of almost all the molecular pairs, except for the stacked dimer in the crystal environment (the PIXEL calculations) were found to be similar to those in isolated state (DFT-D3/B97-D calculations). The molecular stacking was found to be more stabilized in the latter compared to that in the crystal environment.

3. The total interaction energies (lattice energies) of all of the compounds were obtained to be experimentally similar to the sublimation energies [except for **AC-3 (Form I)**].

4. It was observed that there occurs a change in the crystal packing associated with substitution with either fluorine or trifluoromethyl group when compared to the parent compound, thereby signifying the participation of different kinds of stable supramolecular motifs that contribute towards the stability in crystal packing.

5. A very important and significant observation is as follows: It is to be noted that in the case of the parent compounds (**AC-0** and **BZ-0**) the summation of the interaction energies coming from contributions of the "initial" most stable molecular pairs approach the final value of the lattice energy. Interestingly, in the case of their fluoro or trifluoromethyl analogues, this requires the contribution of an increased number of molecular pairs, this resulting from the possibility of increased participation of organic fluorine in different intermolecular interactions in the crystal. Hence it can be concluded that in reality a

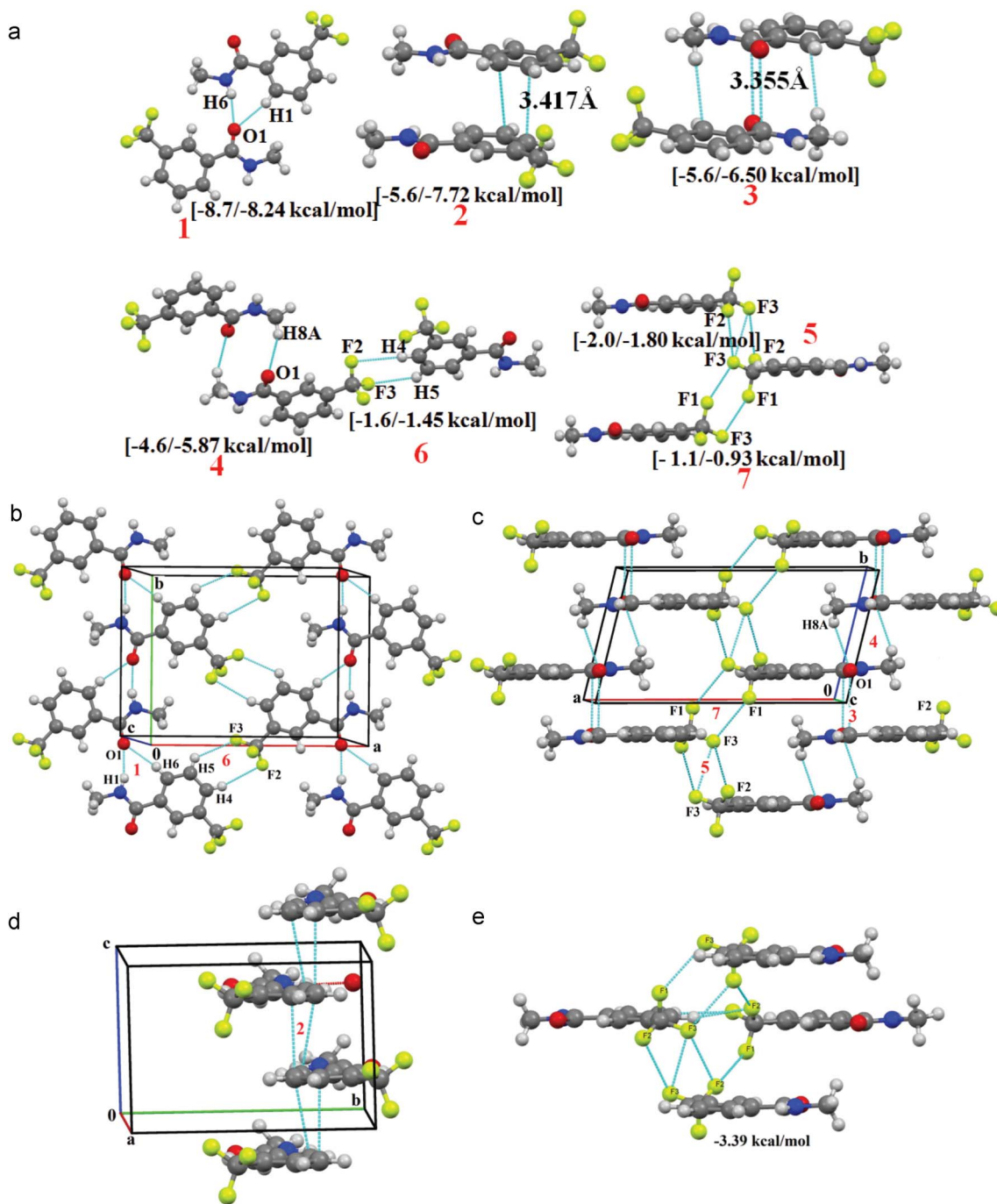


**Fig. 13** (a) Selected molecular pair present in crystal with their interaction energies from PIXEL and DFT-D3 calculation (Table 4) respectively in **BZ-5**. (b) Packing view down the *ab* plane, displaying strong N-H...O=C, weak C-H...O C(sp<sup>2</sup>)-H...F-C(sp<sup>3</sup>) hydrogen bonds in **BZ-5**. (c) Packing view down the *ab* plane, displaying C=O...C=O interactions along with weak C(sp<sup>3</sup>)-H...O hydrogen bonds and C(sp<sup>3</sup>)-F...F-C(sp<sup>3</sup>) interactions in **BZ-5**. (d) Packing molecule down the *bc* plane in **BZ-5**. (e) Tetrameric motif in **BZ-5** depicting C(sp<sup>3</sup>)-F...F-C(sp<sup>3</sup>) and C(sp<sup>2</sup>)-H...F-C(sp<sup>3</sup>).

re-distribution of the total stabilization energy happens amongst the different supramolecular motifs observed in the crystal.

6. The order of interaction energies were observed in most of the cases in descending order of magnitude as follows: motif containing N-H...O, strong H-bonds (-8 to -9 kcal mol<sup>-1</sup>) > molecular stacking (-4 to -7 kcal mol<sup>-1</sup>) > motifs containing

C-H...O (-3 to 5 kcal mol<sup>-1</sup>) > motifs containing mainly interactions involving fluorine (-1 to -3 kcal mol<sup>-1</sup>).

7. A close analysis of the energetics of different molecular pairs involving hydrogen bonds with fluorine (explicitly given in Table S5, ESI†) reveals that motifs containing C(sp<sup>2</sup>)-H...F-C(sp<sup>3</sup>/sp<sup>2</sup>) are more stabilized than those of C(sp<sup>3</sup>)-H...F-C(sp<sup>3</sup>/sp<sup>2</sup>). In addition, it is also observed that C(sp<sup>3</sup>/sp<sup>2</sup>)-

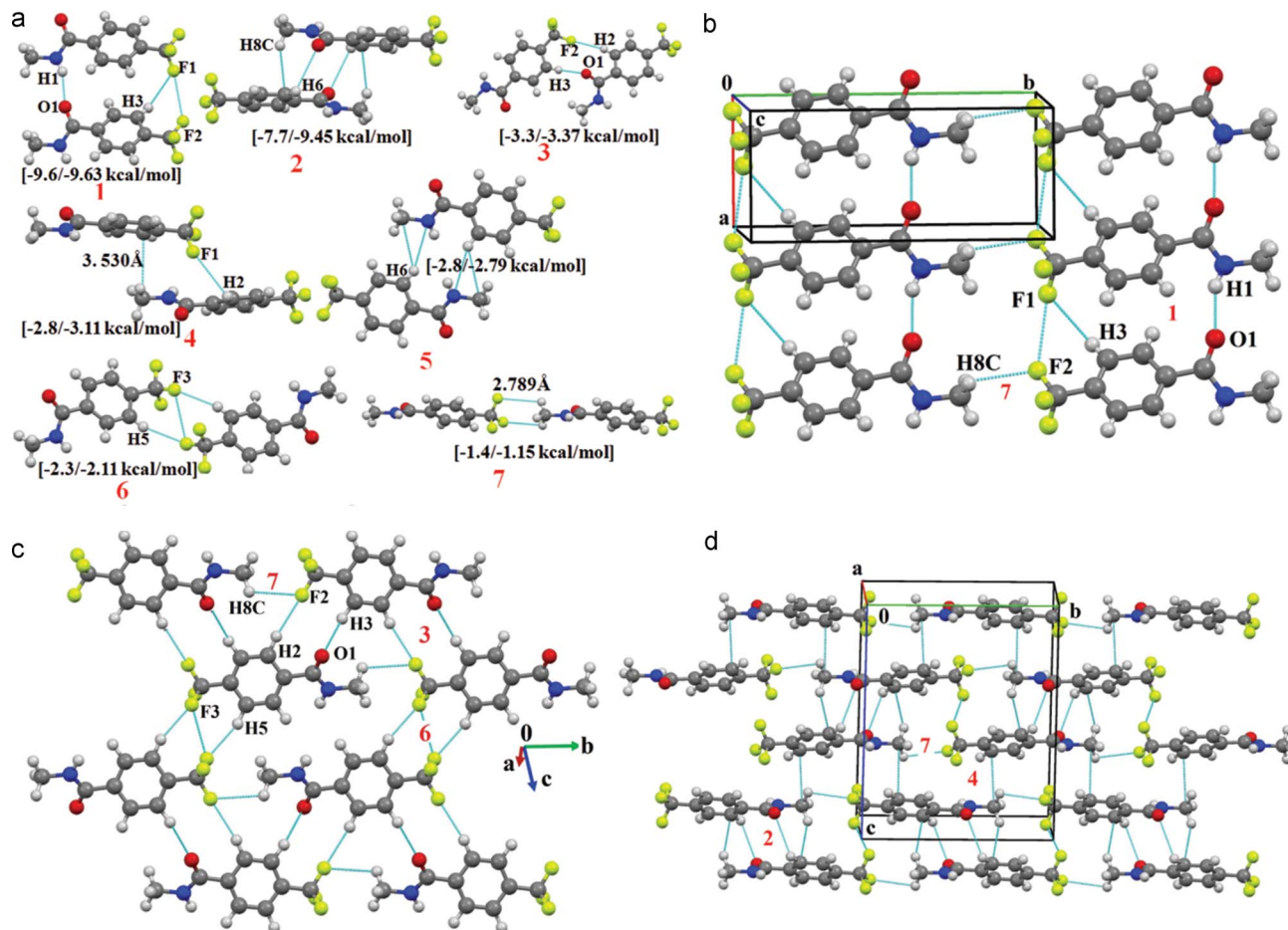


**Fig. 14** (a) Selected molecular pair with their interaction energies calculated from pixel and DFT-D3 calculation (Table 4) in **BZ-6**. (b) Packing view depicting the formation of molecular sheets down the *ab* plane via strong N-H...O=C, weak C(sp<sup>2</sup>)-H...F-C(sp<sup>3</sup>) hydrogen bonds and C(sp<sup>3</sup>)-F...F-C(sp<sup>3</sup>) interactions in **BZ-6**. (c) Packing view depicting formation of sheets via weak C-H...O, C(sp<sup>2</sup>)-H...F-C(sp<sup>3</sup>) and C(sp<sup>3</sup>)-H...F-C(sp<sup>3</sup>) hydrogen bonds in **BZ-6**. (d) Packing of **BZ-6** down the *bc* plane, showing formation of layers via weak C-C(sp<sup>2</sup>)-H...O, C(sp<sup>3</sup>)-H...π hydrogen bonds and C(sp<sup>3</sup>)-F...F-C(sp<sup>3</sup>) interactions.

H...F-C(sp<sup>3</sup>) are more stabilized than those in C(sp<sup>3</sup>/sp<sup>2</sup>)-H...F-C(sp<sup>2</sup>). This indicates that fluorine connected to sp<sup>3</sup> hybridized carbon has greater propensity of forming H-bonds.

## Conclusions

The synthesis, crystallographic investigations and quantitative estimation of the energetic contributions of different “key” supramolecular motifs, particularly those involving organic fluorine in the context of crystal packing has been established in the manuscript. In addition to the significance of the coulombic nature of strong N-H...O=C and C-H...O=C H-bonds, the stabilizing role of stacking interactions along with the dispersive nature of C-H...F H-bonds and related interactions involving fluorine has been realized in these library of molecules. Contributions from fluorine interactions are significant and do contribute towards the overall stability of the crystal packing. It is now of interest to extend this evaluation of the energetic contribution of interactions involving organic fluorine in related complex molecules

constituted of the basic functional groups that are present in the current scheme of molecules. This will enable an improved understanding of such weak interactions, particularly those involving organic fluorine and enable an identification of “recurring” molecular pairs which are present as key building blocks in the crystal structure. To summarize, a complete understanding of fluorine interactions has still not been achieved and extended investigations in different molecules is of importance and of focus.

## Acknowledgements

The authors thank IISER Bhopal for research and instrument facilities. PP acknowledges the help from Mahesh, IISER Mohali for discussions related to PIXEL calculations and UGC for JRF-SRF funding. We thank Dr V. Srinivasan for help in the theoretical calculations related to TURBOMOLE. DC thanks the DST-Fast track scheme 2010 for funding.

## References

- 1 F. H. Allen, *Acta Crystallogr.*, 2002, **B58**, 380.
- 2 D. Chopra and T. N. Guru Row, *J. Indian Inst. Sci.*, 2007, **87**(2), 169.
- 3 (a) J. D. Dunitz and A. Gavezzotti, *Cryst. Growth Des.*, 2012, **12**, 5873; (b) L. Maschio, B. Civalleri, P. Ugliengo and A. Gavezzotti, *J. Phys. Chem. A*, 2011, **115**, 11179; (c) J. D. Dunitz and A. Gavezzotti, *Chem. Soc. Rev.*, 2009, **38**, 2622; (d) A. Gavezzotti, *J. Pharm. Sci.*, 2007, **96**, 2232; (e) J. D. Dunitz and A. Gavezzotti, *Cryst. Growth Des.*, 2005, **5**, 2180; (f) J. D. Dunitz and A. Gavezzotti, *Angew. Chem., Int. Ed.*, 2005, **44**, 1766; (g) L. Carlucci and A. Gavezzotti, *Chem.–Eur. J.*, 2005, **11**, 271; (h) A. Gavezzotti, *CrystEngComm*, 2003, **5**, 429; (i) A. Gavezzotti, *CrystEngComm*, 2003, **5**, 439.
- 4 (a) G. R. Desiraju, *Angew. Chem., Int. Ed.*, 2011, **50**, 52; (b) E. Arunan, G. R. Desiraju, R. A. Klein, J. Sadlej, S. Scheiner, I. Alkorta, D. C. Clary, R. H. Crabtree, J. J. Dannenberg, P. Hobza, H. G. Kjaergaard, A. C. Legon, B. Mennucci and D. J. Nesbitt, *Pure Appl. Chem.*, 2011, **83**, 1619.
- 5 (a) M. Nishio, Y. Umezawa, K. Honda, S. Tsuboyama and H. Suezawa, *CrystEngComm*, 2009, **11**, 1757; (b) O. Takahashi, Y. Kohno and M. Nishio, *Chem. Rev.*, 2010, **110**, 6049; (c) M. Nishio, *Phys. Chem. Chem. Phys.*, 2011, **13**, 13873.
- 6 P. Munshi, *PhD thesis*, Indian Institute of Science, Bangalore, 2005.
- 7 (a) D. Chopra, K. Nagarajan and T. N. Guru Row, *Cryst. Growth Des.*, 2005, **5**, 1035; (b) G. Cavallo, P. Metrangolo, T. Pilati, G. Resnati, M. Sansotera and G. Terraneo, *Chem. Soc. Rev.*, 2010, **39**, 3772; (c) A. R. Choudhury and T. N. Guru Row, *Cryst. Growth Des.*, 2004, **4**, 47.
- 8 (a) S. Kawahara, S. Tsuzuki and T. Uchimaru, *J. Phys. Chem. A*, 2004, **108**, 6744; (b) I. Saraogi, V. G. Vijay, S. Das, K. Sekar and T. N. Guru Row, *CrystEngComm*, 2003, **6**, 69; (c) M. D. Prasanna and T. N. Guru Row, *CrystEngComm*, 2000, **3**, 135.
- 9 (a) V. R. Hathwar, R. G. Gonnade, P. Munshi, M. M. Bhadbhade and T. N. Guru Row, *Cryst. Growth Des.*, 2011, **11**, 1855; (b) V. R. Hathwar and T. N. Guru Row, *Cryst. Growth Des.*, 2011, **11**, 1338; (c) V. R. Hathwar and T. N. Guru Row, *J. Phys. Chem. A*, 2010, **114**, 13434.
- 10 J. D. Dunitz, *ChemBioChem*, 2004, **5**, 614.
- 11 K. Reichenbacher, H. I. Suss and J. Hulliger, *Chem. Soc. Rev.*, 2005, **34**, 22.
- 12 H.-J. Schneider, *Chem. Sci.*, 2012, **3**, 1381.
- 13 R. Berger, G. Resnati, P. Metrangolo, E. Weber and J. Hulliger, *Chem. Soc. Rev.*, 2011, **40**, 3496 and references therein.
- 14 D. Chopra and T. N. Guru Row, *CrystEngComm*, 2011, **13**, 2175 and references therein.
- 15 V. Gouverneur, K. Muller and F. Diederich, *Fluorine in Pharmaceutical and Medicinal Chemistry: From Biophysical Aspects to Clinical Applications*, World Scientific Publishing, Company, London, 2012.
- 16 D. Chopra, *Cryst. Growth Des.*, 2012, **12**, 541.
- 17 D. Chopra, T. S. Cameron, J. D. Ferrara and T. N. Guru Row, *J. Phys. Chem. A*, 2006, **110**, 10465.
- 18 G. Kaur, P. Panini, D. Chopra and A. R. Choudhury, *Cryst. Growth Des.*, 2012, **12**, 5096.
- 19 V. Vasylyrva, O. V. Shishkin, A. V. Maleev and K. Merz, *Cryst. Growth Des.*, 2012, **12**, 1032.
- 20 (a) D. Chopra and T. N. Guru Row, *CrystEngComm*, 2008, **10**, 54; (b) S. K. Nayak, M. K. Reddy, T. N. Guru Row and D. Chopra, *Cryst. Growth Des.*, 2011, **11**, 1578; (c) P. Panini and D. Chopra, *CrystEngComm*, 2012, **14**, 1972.
- 21 (a) H. J. Wasserman, R. R. Ryan and S. P. Layne, *Acta Crystallogr.*, 1985, **C41**, 783; (b) S. W. Johnson, J. Eckert, M. Barthes, R. K. McMullan and M. Muller, *J. Phys. Chem.*, 1995, **99**, 16253.
- 22 L. Leiserowitz and M. Tuval, *Acta Crystallogr.*, 1978, **B34**, 1230.
- 23 (a) N. P. Sahu, C. Pal, N. B. Mandal, S. Banerjee, M. Raha, A. P. Kundu, A. Basu, M. Ghosh, K. Roy and S. Bandyopadhyay, *Bioorg. Med. Chem.*, 2002, **10**, 1687–1693; (b) R. G. Sherrill, J. M. Berman, L. Birkemo, D. K. Croom, M. Dezube, G. N. Ervin, M. K. Grizzle, M. K. James, M. F. Johnson, K. L. Queen, T. J. Rimele, F. Vanmiddlesworth and E. E. Sugg, *Bioorg. Med. Chem. Lett.*, 2001, **11**, 1145.
- 24 C. Nichols and C. S. Frampton, *J. Pharm. Sci.*, 1998, **87**, 684.
- 25 A. Altomare, G. Cascarano, C. Giacovazzo and A. Guagliardi, *J. Appl. Crystallogr.*, 1993, **26**, 343.
- 26 G. M. Sheldrick, *Acta Crystallogr.*, 2008, **A64**, 112.
- 27 L. J. Farrugia, WinGx, *J. Appl. Crystallogr.*, 1999, **32**, 837.
- 28 L. J. Farrugia, *J. Appl. Crystallogr.*, 1997, **30**, 565.
- 29 C. F. Macrae, I. J. Bruno, J. A. Chisholm, P. R. Edgington, P. McCabe, E. Pidcock, L. Rodriguez-Monge, R. Taylor, J. Streek and P. A. Wood, *J. Appl. Crystallogr.*, 2008, **41**, 466, [www.ccdc.cam.ac.uk/mercury](http://www.ccdc.cam.ac.uk/mercury).
- 30 M. Nardelli, *J. Appl. Crystallogr.*, 1995, **28**, 569.
- 31 A. L. Spek, *Acta Crystallogr.*, 2009, **D65**, 148.
- 32 S. K. Nayak, M. K. Reddy, D. Chopra and T. N. Guru Row, *CrystEngComm*, 2012, **14**, 200.
- 33 (a) R. Ahlrichs, M. Baer, M. Haeser, H. Horn and C. Koelmel, Electronic structure calculations on workstation computers: the program system TURBOMOLE, *Chem. Phys. Lett.*, 1989, **162**, 165–169; (b) TURBOMOLE V6.3 2011, a development of University of Karlsruhe and Forschungszentrum Karlsruhe GmbH, 1989–2007, TURBOMOLE GmbH, since 2007, available from <http://www.turbomole.com>.
- 34 (a) A. Gavezzotti, *New J. Chem.*, 2011, **35**, 1360; (b) A. Gavezzotti, *J. Phys. Chem. B*, 2003, **107**, 2344; (c) A. Gavezzotti, *J. Phys. Chem. B*, 2002, **106**, 4145.
- 35 M. J. Frisch, G. W. Trucks, H. B. Schlegel, G. E. Scuseria, M. A. Robb, J. R. Cheeseman, G. Scalmani, V. Barone, B. Mennucci, G. A. Petersson, H. Nakatsuji, M. Caricato, X. Li, H. P. Hratchian, A. F. Izmaylov, J. Bloino, G. Zheng, J. L. Sonnenberg, M. Hada, M. Ehara, K. Toyota, R. Fukuda, J. Hasegawa, M. Ishida, T. Nakajima, Y. Honda, O. Kitao, H. Nakai, T. Vreven, J. A. Montgomery Jr., J. E. Peralta, F. Ogliaro, M. Bearpark, J. J. Heyd, E. Brothers, K. N. Kudin, V. N. Staroverov, R. Kobayashi, J. Normand, K. Raghavachari, A. Rendell, J. C. Burant, S. S. Iyengar, J. Tomasi, M. Cossi, N. Rega, J. M. Millam, M. Klene, J. E. Knox, J. B. Cross, V. Bakken, C. Adamo, J. Jaramillo, R. Gomperts, R. E. Stratmann, O. Yazyev, A. J. Austin, R. Cammi, C. Pomelli, J. W. Ochterski, R. L. Martin, K. Morokuma, V. G. Zakrzewski, G. A. Voth, P. Salvador, J. J. Dannenberg, S. Dapprich, A. D. Daniels, Ö. Farkas, J. B. Foresman, J. V. Ortiz, J. Cioslowski and D. J. Fox, *Gaussian 09, Revision A.02*, Gaussian, Inc., Wallingford CT, 2009.
- 36 (a) S. Grimme, J. Antony, S. Ehrlich and H. Krieg, *J. Chem. Phys.*, 2010, **132**, 154104; (b) J. Moellmann and S. Grimme,

- Phys. Chem. Chem. Phys.*, 2010, **12**, 8500; (c) W. Hujo and S. Grimme, *Phys. Chem. Chem. Phys.*, 2011, **13**, 13942.
- 37 S. Grimme, *J. Comput. Chem.*, 2006, **27**, 1787.
- 38 D.-C. Li, W.-Y. Zhou and C.-B. Li, *Acta Crystallogr.*, 2009, **E62**, o66.
- 39 P. Umnahanant and J. Chickos, *J. Chem. Eng. Data*, 2012, **57**, 1331.
- 40 (a) A. Gavezzotti, *J. Phys. Chem.*, 1990, **94**, 4319; (b) F. H. Allen, C. A. Baalham, J. P. M. Lommerse and P. R. Raithby, *Acta Crystallogr.*, 1998, **B54**, 320.
- 41 (a) C. Jackel, M. Salwiczek and B. Kokschi, *Angew. Chem., Int. Ed.*, 2006, **45**, 4198; (b) O. Jeannin and M. Fourmigue, *Chem.-Eur. J.*, 2006, **12**, 2994.